BUDAPEST UNIVERSITY OF TECHNOLOGY AND ECONOMICS
DEPARTMENT OF STRUCTURAL ENGINEERING

TYPE TESTING OF BUCKLING RESTRAINED BRACES ACCORDING TO EN 15129

EWC800

FINAL REPORT

László Dunai D.Sc.
Professor
Head of Department

Contributors:

Ádám Zsarnóczay M.Sc., Ph.D. Student
László Kaltenbach, Academic Associate
Miklós Kálló Ph.D., Honorary Associate Professor
Mansour Kachichian, Assistant Lecturer
Attila Halász, Technician

BUDAPEST, 15TH MARCH 2011

EXECUTIVE SUMMARY

The objective of this report is to analyse and evaluate the performance of buckling restrained braces by type tests using methodology proposed in European standards, specifically in EN 15129. Two braces were tested; both manufactured by Star Seismic Europe Ltd. Tests were performed at the Structural Laboratory of the Department of Structural Engineering at the Budapest University of Technology and Economics at the end of 2010.

The yielding zone of the steel core of test specimens has a cross-sectional area of 800mm^2, the actual cross-section resistance (yielding point) of test specimens is 225 kN. The testing protocol is a combination of the protocols specified by EN 15129 and ECCS, exceeding the requirements of both documents. A total of more than 65 load cycles were performed with at least 30 cycles at design displacement level. Both specimens completed the protocol without any sign of premature failure or damage during the prescribed cycles.

Both specimens showed a stable hysteretic behaviour with significant energy dissipation capabilities and cyclic hardening. Maximum inelastic deformations exceeded 10 times the deformation at first significant yield during cyclic loading. Deformation capacity of the tested specimen is more than 1.7 times the design displacement. All applicable requirements found in the EN 15129 standard are met by the specimens and explained in detail in this document. Both specimens were disassembled after failure. Findings during disassembly verify that the working mechanism is in good agreement with theoretical expectations.

TABLE OF CONTENTS

LIST OF TABLES

List of Figures

LIST OF SYMBOLS

Roman

b	braced frame bay width
d	general symbol for displacement
d_1	yield displacement as per EN 15129
d_{bd}	design displacement
d_{max}	maximum displacement experienced
d_r	interstory drift
d_{ya}	actual yield displacement
d_y*	yield displacement as per ECCS
$f_{ua,c}$	actual ultimate strength of the material of the steel core
$f_{ua,s}$	actual ultimate strength of the material of the subassembly structure
$f_{uk,c}$	characteristic ultimate strength of the material of the steel core
$f_{uk,s}$	characteristic ultimate strength of the material of the subassembly structure
$f_{ya,c}$	actual yield strength of the material of the steel core
$f_{ya,s}$	actual yield strength of the material of the subassembly structure
$f_{yk,c}$	characteristic yield strength of the material of the steel core
$f_{yk,s}$	characteristic yield strength of the material of the subassembly structure
h	braced frame bay height
l_e	length of the elastic zone of the steel core
l_s	length of the subassembly structure
l_t	length of the transition zone of the steel core
l_y	length of the yielding zone of the steel core
t_e	thickness of the steel core in the elastic zone
t_s	thickness of the subassembly structure
t_y	thickness of the steel core in the yielding zone
w_e	width of the steel core in the elastic zone
w_s	width of the subassembly structure
w_y	width of the steel core in the yielding zone
A_e	cross-sectional area of the steel core in the elastic zone
A_s	cross-sectional area of the subassembly structure
A_y	cross-sectional area of the steel core in the yielding zone
E_h	total dissipated hysteretic energy
$F_{ac,c}$	actual cross-section resistance
F_y	general symbol for yield force
F_y*	yield force as per ECCS
$K_{1,C}$	first branch stiffness under compression
$K_{1,T}$	first branch stiffness under tension

$K_{2,C}$	second branch stiffness under compression
$K_{2,T}$	second branch stiffness under tension
K_{effb}	effective stiffness
L	maximum wp-wp length of a BRB in a braced frame under design seismic excitation
L_0	initial wp-wp length of a BRB in a braced frame
V_1	yield force as per EN 15129
V_{bd}	general symbol for design force value
$V_{Ebd,C}$	design force value under compression
$V_{Ebd,T}$	design force value under tension
W(d)	work done in a load cycle with amplitude d

Greek

α	inclination of the BRB in the braced frame
α_y	angle that defines the initial slope of the force-displacement relationship
β	compression strength adjustment factor
γ_b	partial factor for design of displacement dependent devices
γ_{ov}	overstrength factor
γ_x	partial factor for design of displacement dependent devices
δ	angle that expresses the maximal (rotational part of) deviation of the BRB from its original position under design seismic excitation
$\varepsilon_{cy,max}$	maximal strain in the yielding zone of the steel core
$\varepsilon_{eq,max}$	equivalent maximal strain determined for the wp-wp length of the specimen
$\varepsilon_{ua,c}$	actual ultimate strain in the steel core
$\varepsilon_{ua,s}$	actual ultimate strain in the subassembly structure
η	cumulative inelastic deformation capacity
$\varkappa$	variation in K_2 relative to the 3rd cycle
ξ_{effb}	equivalent viscous damping value
Ξ	variation in ξ_{effb} relative to the 3rd cycle
ω	tension strength adjustment factor

Abbreviations

AISC	American Institute of Steel Construction
BRB	Buckling Restrained Brace
BRBF	Buckling Restrained Braced Frame
EWC800A	European WildCat 800mm² cross-sectional area A specimen
EWC800B	European WildCat 800mm² cross-sectional area B specimen
ECCS	European Convention for Constructional Steelwork
FEMA	Federal Emergency Management Agency
NLD	Non Linear Device
TBC	Theoretical Bilinear Cycle
wp-wp	workpoint-to-workpoint

1. INTRODUCTION

The concept of Buckling Restrained Braces (BRBs) was developed in Japan at the end of the 1980s. It appeared in the United States after the Northridge earthquake in 1994 and it is now accepted with its design regulated in current standards as a displacement dependent lateral load resisting solution. As earthquake awareness among engineers is enhanced by the European standards, the need for economical solutions providing adequate resistance for new structures is also increasing in Europe. Design or testing of BRBF systems is not addressed in the current version of Eurocode 8 [1], however EN 15129 [2], a separate document on anti-seismic devices does include BRBs. Therefore this report was made using the provisions and specifications of the latter standard.

BRBs are composed of a slender steel core continuously supported by a concrete casing in order to prevent buckling under axial compression. The core and the casing are decoupled to prevent interaction between them. Star Seismic Europe Ltd. uses air gaps for this purpose. When subjected to cyclic loading – since buckling is prevented – the performance of BRB elements is not limited by cyclic degradation due to stability failure. Axial loads are resisted by the inner steel core only and the so called yielding zone of this element is designed to ensure a balanced and stable highly ductile behaviour.

The objective of the current study is to analyse and evaluate the performance of buckling restrained braces by type tests using methodology proposed in European standards, specifically in EN 15129. This provides basis for comparison of test results in the United States and Europe and by that can facilitate the acceptance and standardization of the BRBF system in Europe. Two braces provided by Star Seismic Europe Ltd. were tested using uniaxial cyclic loading protocols at the Structural Laboratory of the Budapest University of Technology and Economics.

2. TEST PROGRAM

2.1. BRACE CHARACTERISTICS

Star Seismic Europe Ltd. provided two identical Buckling Restrained Braces for the tests. Tested BRBs are designated as EWC800A and EWC800B in this report corresponding to the cross-sectional area of the yielding zone of the steel core in mm². EWC refers to the WildCat family of BRBs at Star Seismic Europe Ltd. with welded connections at the ends of the braces.

BRBs are assumed Non Linear Devices (NLD) and therefore classified as Displacement Dependent Devices in EN 15129 3.4. This assumption is verified by evaluating the effective damping of the devices in Section 4.3.6. Figure 1 shows a schematic of tested BRBs and Table 1 gives a summary of important parameters for the highlighted parts. All of the data in Table 1 had been provided by Star Seismic Europe Ltd. Detailed drawings – also provided by Star Seismic Europe Ltd. – are included in Appendix A.

Material of the steel core was examined by an independent accredited testing laboratory (AGMI Material Testing and Quality Management Pte Co. Ltd.) using tensile tests according to MSZ EN 10002-1 [3]. Material of the subassembly structure was analysed by the manufacturer (U.S. Steel Serbia d.o.o.). Detailed results of both tests are included in Appendix B.

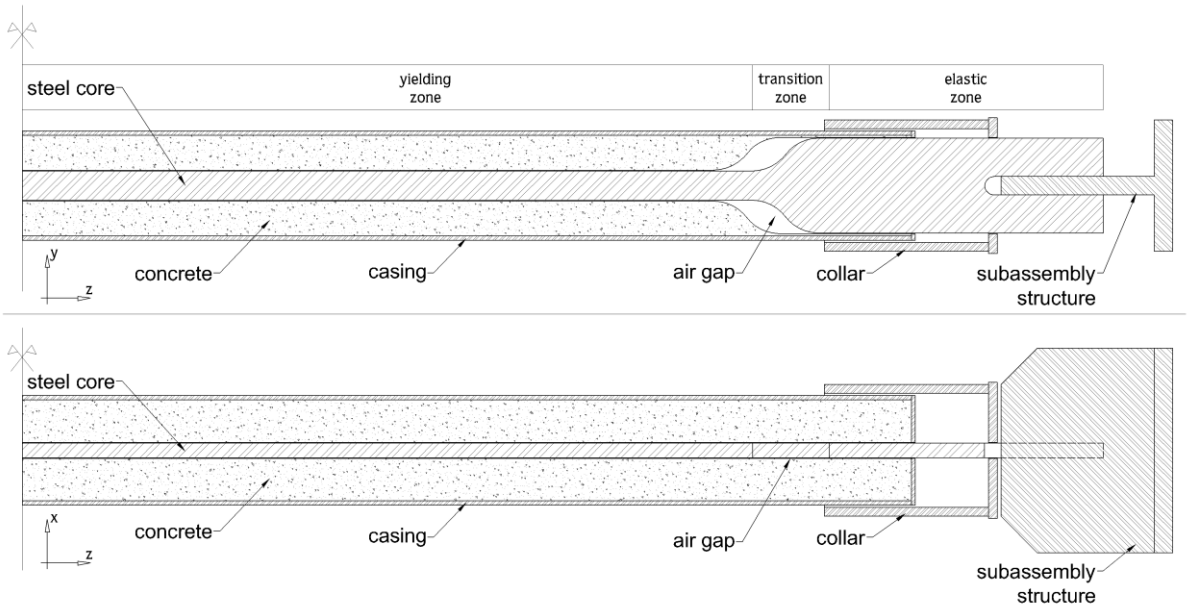

Figure 1 – Longitudinal sections showing the main parts of tested Buckling Restrained Braces

Table 1 – Main attributes of tested Buckling Restrained Braces

				Brace Type
				EWC800
Steel Core	Material Type			S235 JR
		Yield Strength actual ($f_{ya,c}$) / characteristic ($f_{yk,c}$)	[N/mm²]	282 / 235
		Ultimate Tensile Strength actual ($f_{ua,c}$) / characteristic ($f_{uk,c}$)	[N/mm²]	450 / 360
		Maximum Elongation actual ($\varepsilon_{ua,c}$)	[%]	36
	Yielding zone	Thickness t_y	[mm]	20
		Width w_y	[mm]	40
		Area A_y	[mm²]	800
		Length l_y	[mm]	2000
	Transition zone	Length l_t	[mm]	90
	Elastic zone	Thickness t_e	[mm]	20
		Width w_e	[mm]	130
		Area A_e	[mm²]	2600
		Length l_e	[mm]	390
Subassembly Structure	Material Type			S355 J2C
		Yield Strength actual ($f_{ya,s}$) / characteristic ($f_{yk,s}$)	[N/mm²]	436 / 355
		Ultimate Tensile Strength actual ($f_{ua,s}$) / characteristic ($f_{uk,s}$)	[N/mm²]	578 / 470
		Maximum Elongation actual ($\varepsilon_{ua,s}$)	[%]	25
	Thickness t_s		[mm]	25
	Width w_s		[mm]	280
	Area A_s		[mm²]	7000 (4500)
	Length l_s		[mm]	160 (210)

2.2. DESIGN DISPLACEMENT

As per EN 15129 6.4.4 a) the maximum displacement during cyclic loading shall be at least equal to the design displacement of the device, d_{bd}, which is defined in EN 15129 3.1.4 as the total displacement the device is subjected in case of the design seismic action according to EN 1998-1 [1]. Regardless of the seismic action, displacements have an upper limit in order to prevent dangerous levels of interstory drifting. The influence of P-Δ effects increases significantly at large interstory drifts, which leads to unfavourable structural response. Large interstory drift ratios also lead to extensive damage in non-structural elements of buildings. According to EN 1998-1 4.4.3.2 the maximum interstory drift ratio allowed under design seismic action associated with the damage limitation requirement (95 year return period) is 1%. Considering the lower return period of such earthquakes and taking into account the possibility of a 475 year return period seismic action, the maximum interstory drift ratio to be considered as per EN 1998-1 4.4.3.2 is 2% for ordinary structures. Therefore instead of defining an arbitrary frame structure for the tested BRBs (which would include a considerable amount of uncertainty), specimens are tested for the maximum possible displacement level regardless of the actual structure they might be used in.

The only assumption made during the following calculation is that the inclination of the braces is 45°. Figure 2 shows such a brace configuration with geometric details expressed as a function of brace workpoint-to-workpoint (wp-wp) length L (i.e. the distance between the midpoints of the joints the brace is connected to). As it is pointed out on Figure 2, the design displacement of a BRB with 45° inclination in case of the maximal 2% interstory drift ratio can be considered equal to 1% of its wp-wp length.

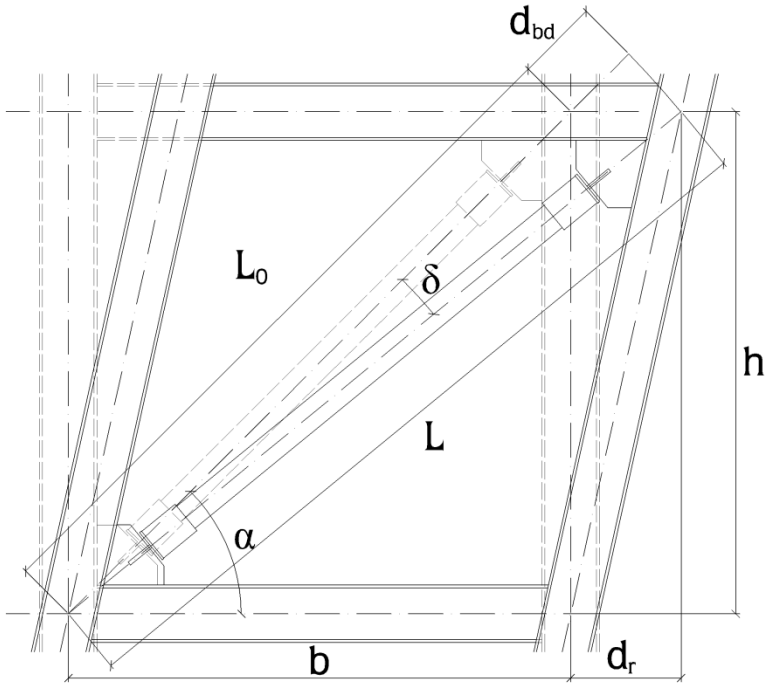

$$h = L_0 sin\alpha$$
$$b = L_0 cos\alpha$$
$$L = \sqrt{(h^2) + (b + d_r)^2}$$
$$\delta = \alpha - arctg\left(\frac{h}{b + d_r}\right)$$

$in\ case\ of\ 2\%\ interstory\ drift$:
$$d_r = 0.02 \cdot h$$

$if\ \alpha = 45^o$:
$$h = \frac{L_0}{\sqrt{2}} \qquad b = \frac{L_0}{\sqrt{2}}$$
$$L = 1.01005 \cdot L_0$$

$$d_{bd} = L - L_0 = 0.01005 \cdot L_0$$
$$d_{bd} \cong 0.01 \cdot L_0$$

$$\delta = \frac{\pi}{4} - arctg\left(\frac{50}{51}\right) = 0.0099$$
$$\delta \cong 0.567^o$$

Figure 2 – Determination of design displacement for BRB elements in frames affected by design seismic action

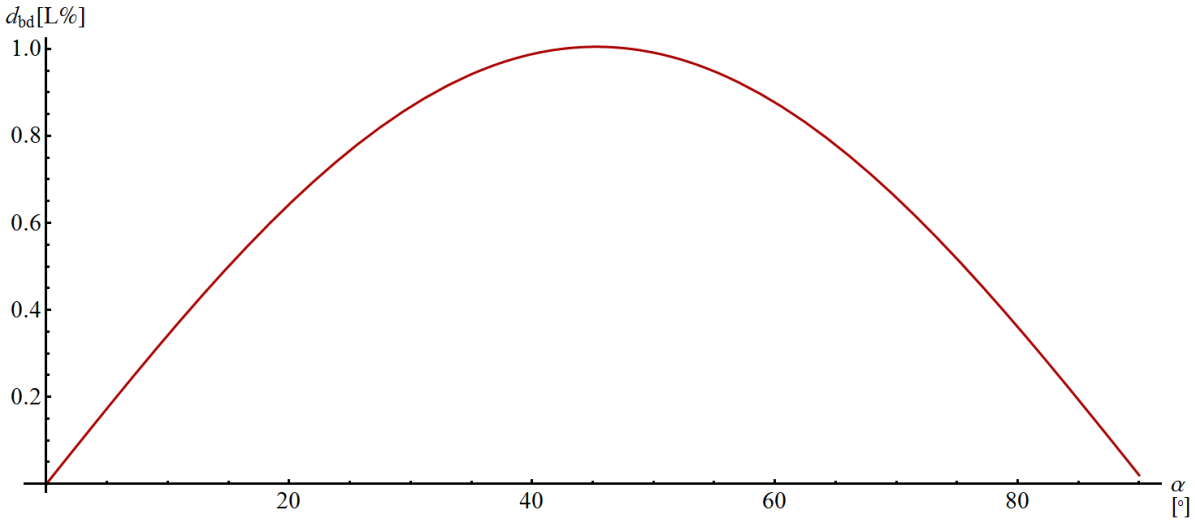

Figure 3 – Magnitude of design displacement for different BRB configurations subjected to 2% interstory drift ratio

The resulting design displacement for braces with different inclinations is shown on Figure 3. Accordingly, by using 1% of brace wp-wp length, specimens in this test are subjected to the maximum possible displacement level as per EN 1998-1 4.4.3.2. Considering that the total length of tested BRB specimens including subassembly structures is 3.140 m, a maximum wp-wp length of 4.000 m is assumed. This results in a design displacement of 40 mm.

The above design displacement accompanies rotation of the BRB around its fixings. In other words: the inclination of the braces (α) changes during an earthquake event with the movement of the structure. Since BRBs of this type test are designed with welded connections, their rotation is impeded and this results in second order moments that shall be taken into account during type testing as per EN 15129 6.4.4. Second order moments are proportional to the change in inclination, δ. The maximum level of δ occurs at the maximum displacement level, which is the design displacement, d_{bd}. At this point, the rotation of braces equals to 0.567° (see Figure 2).

2.3. TESTING EQUIPMENT

A schematic of the testing setup is shown on Figure 4, while a picture made during the test is shown on Figure 7. Braces are kept in a quasi-vertical position and bolted to the testing frame using the subassembly structures designed, welded and provided by Star Seismic Europe Ltd. (see Appendix A for detailed drawings and Table 1 for characteristics). The upper part of the frame houses a Schenk 250 kN load cell (Figure 5). The lower part of the frame includes a total of three hydraulic jacks and the necessary subassembly structures (Figure 8). Compressive and tensile loading is generated by a single Frieseke & Hoepfner LZM 40/200 hydraulic jack and two Frieseke & Hoepfner LZM 25/200 hydraulic jacks respectively. Hydraulic jacks are regulated by Mannesmann Rexroth 283/98/40 and Frieseke & Hoepfner RKA 7/1,6 F4 R450 hydraulic pumps with manual control. All load cycles prior yielding are force controlled, the ones post yielding are displacement controlled.

EN 15129 6.4.4 requires displacement dependent devices to be tested together with their connection system under circumstances that reproduce working conditions and fixings of the device. Therefore – in order to take the effect of second order moments on endings of the braces into account as mentioned in Section 2.2 – braces are taken out of plumb by displacing their lower end horizontally by 50 mm. Considering the length of the braces and subassembly structures, this displacement equals to 0.912° rotation, which exceeds the rotation due to deformed frame geometry under seismic action shown on Figure 2 (0.567°). Therefore the effect of frame deformation and resulting second order moments are taken appropriately into account.

2.4. MEASUREMENT DEVICES

Several attributes of the tests are measured as shown on Figure 7. The load cell inserted to the top of the testing frame (Figure 6) measures the total load in the specimen. Taking into account that the braces are taken out of plumb, the axial load in the BRB is 99.99% of the total load measured, therefore these two quantities are considered identical in this report. Transversal load in the braces is 1.59% of the total load. Bending moment generated by this latter load is taken into account during the evaluation of results.

The deformation of braces is determined by measuring the displacement of the lower subassembly structure relative to the midpoint of the steel hollow section of the casing (partial deformation, see Figures 11 and 13) and also to the upper subassembly structure (total deformation, see Figures 12 and 14). The partial deformation is recorded to analyse the movement of casing relative to subassembly structures during the experiment. The total deformation is used to calculate the strain levels in each part of the BRB and to describe its hysteretic behaviour during cyclic loading. Displacements are measured with HBM W50 and W100 transducers.

Horizontal displacement of the lower subassembly structure is also recorded to ensure that braces are tested in the desired configuration without any significant variation during the load cycles. Horizontal deformation is measured at the lower subassembly structure relative to the testing frame by an HBM WTA transducer connected to the braces in the vicinity of the bolted joint (Figure 9). Even when subjected to the design displacement, only the core of the BRB element shall experience yielding. All of the other parts are expected to remain elastic. This behaviour is verified by analysing the strain levels using two Kaliber LIAS gauges on the subassembly structure (Figure 10).

Samples from all measurement equipment are taken at a frequency of 2 Hz and saved by a PC connected to the HBM Spider 8 measurement unit. All of the experimental data are later saved in an electronic file and processed separately.

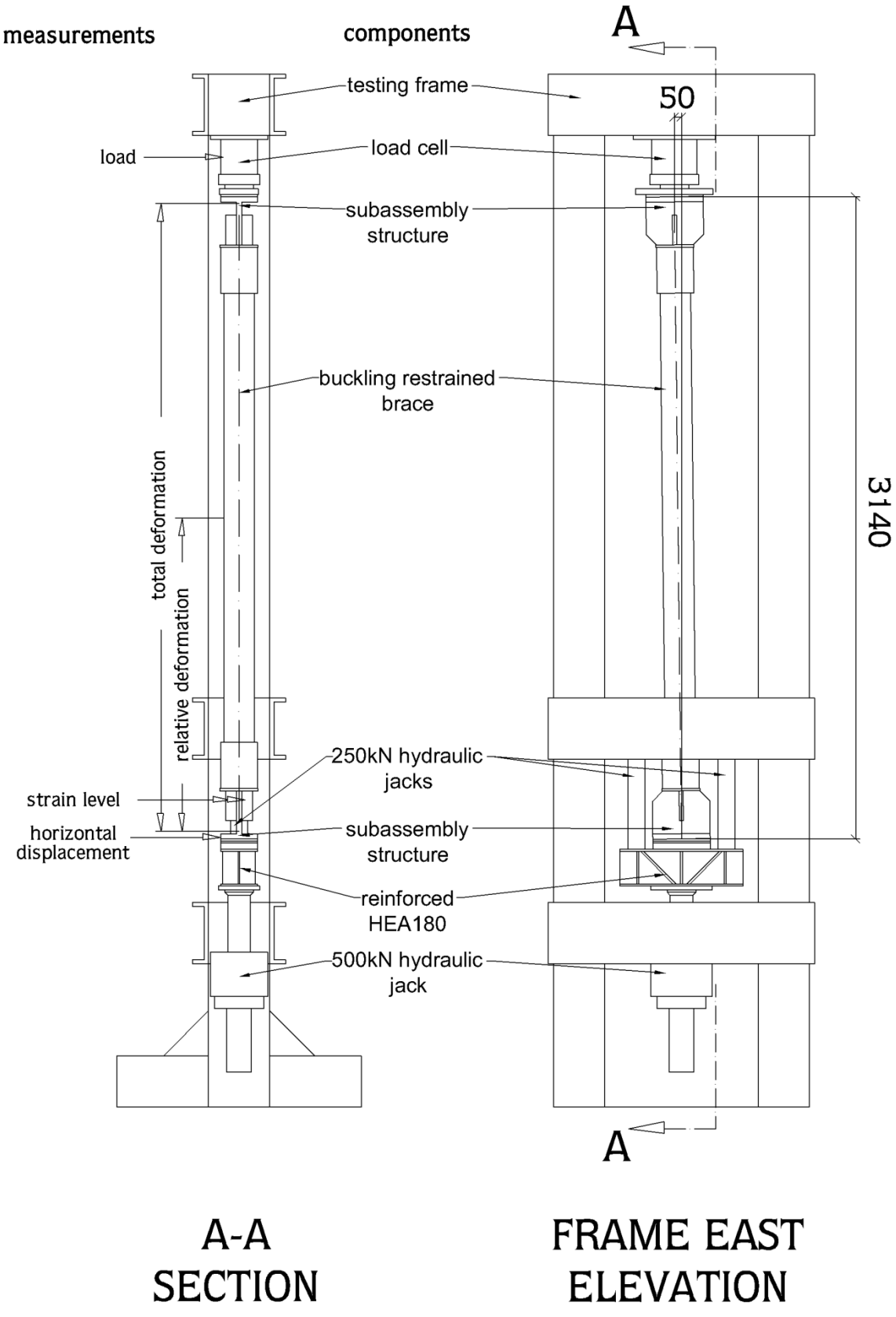

Figure 4 – Schematic of the BRB test setup

Figure 7 – BRB test setup

Figure 5 – Top part of the loading frame

Figure 6 – Load cell

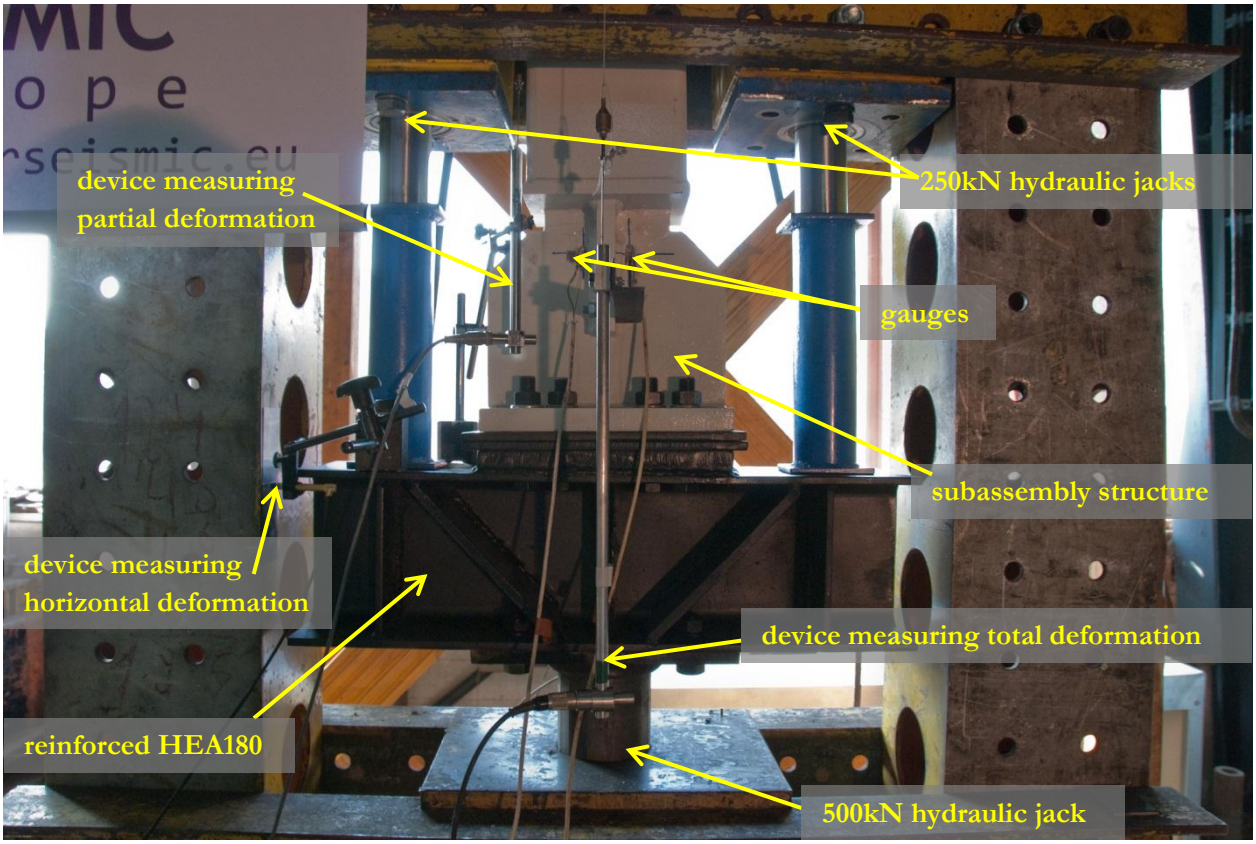

Figure 8 – Bottom part of the loading frame

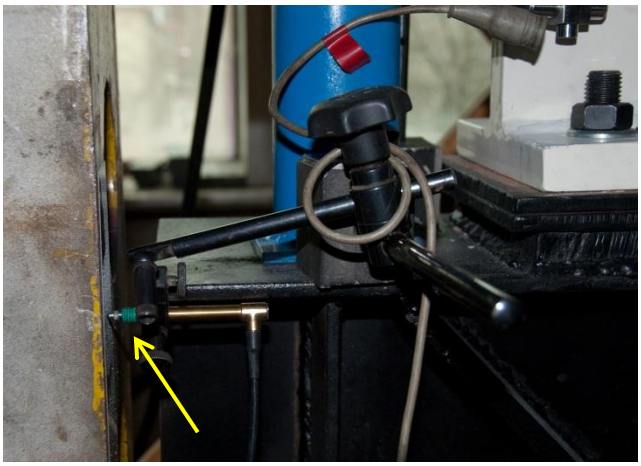

Figure 9 – Device used for measuring horizontal displacement

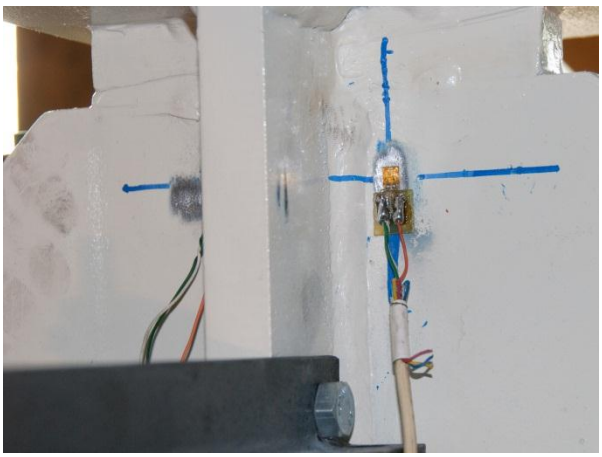

Figure 10 – Gauges installed on the subassembly structure

Figure 11 – Partial axial displacement top

Figure 12 – Full axial displacement top

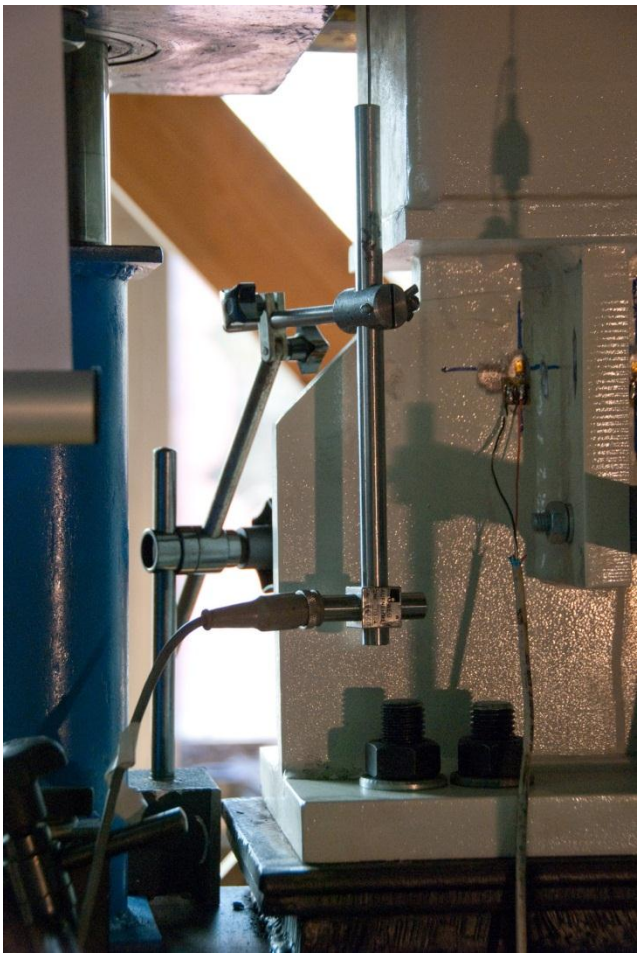

Figure 13 – Partial axial displacement bottom

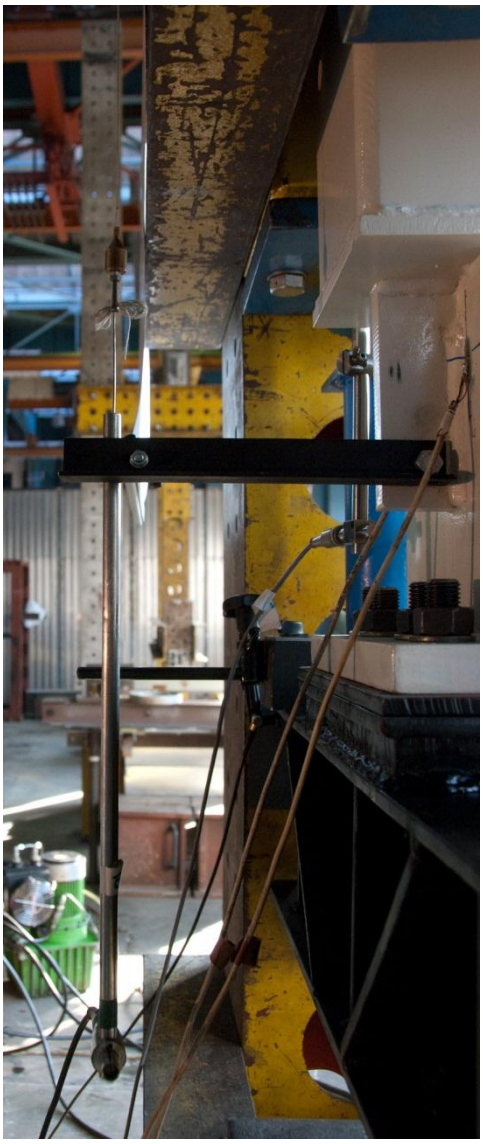

Figure 14 – Full axial displacement bottom

3. LOADING PROTOCOLS

3.1. REQUIREMENTS OF EN 15129

Primary focus during the experiments is on the requirements of EN 15129, specifically on Section 6.4.4. a. The basic test protocol defined is shown on Figure 15. The standard states that the number of test cycles at the design displacement level shall be increased for devices with fundamental periods considerably less than 2s. Structures equipped with BRBF generally have a fundamental period in between 1-2s, therefore an appropriate increase in load cycles is necessary.

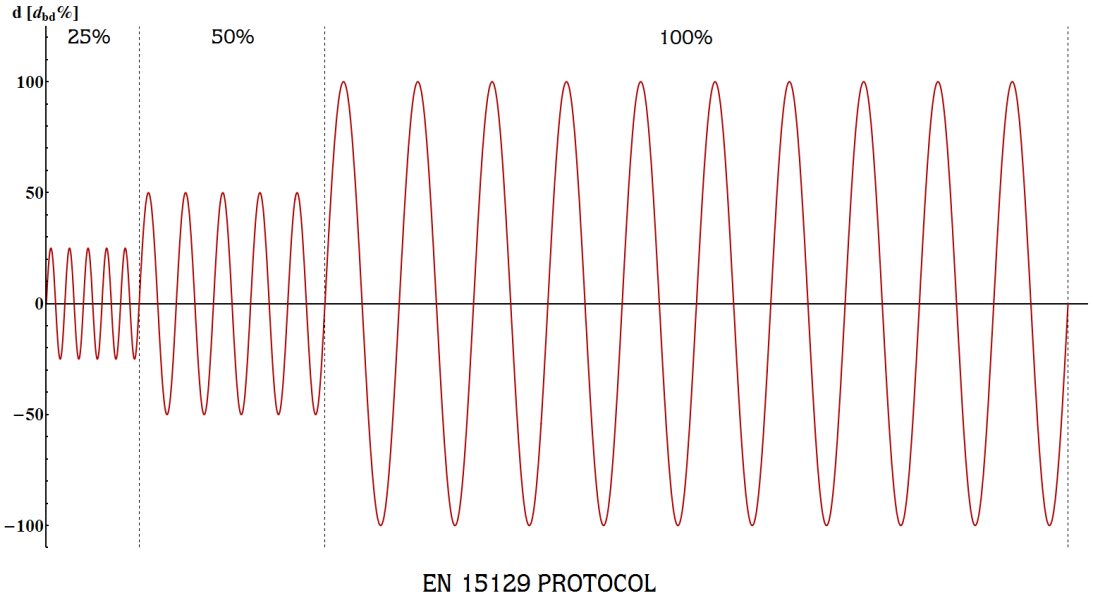

Figure 15 – Loading protocol specified in EN 15129 6.4.4. a

3.2. PROTOCOL PROPOSED BY ECCS

A protocol proposed by the European Convention for Constructional Steelwork (ECCS) for testing structural elements under cyclic loads [4] is also taken under consideration (Figure 16). Unlike the EN 15129 protocol, the amplitude of load cycles depends on the yield displacement (e_y, identical to d_y) in this case. Displacement at yield is defined in [4] as:

$$e_y^+ = \frac{F_y^+}{tg\alpha_y^+} \qquad e_y^- = \frac{F_y^-}{tg\alpha_y^-} \tag{1}$$

where:

$F_y^{+/-}$ is the yield load in the positive/negative force range (for calculation see Section 4.2.1)

$tg\alpha_y^{+/-}$ is the slope of the tangent at the origin of the (F-e) curve, when F increases on the positive/negative side. Identical to the first branch stiffness in EN 15129 (for calculation see Section 4.1)

Yield displacement is estimated using characteristic material properties before the tests and verified after first yield during every experiment. The estimated and actual values show good agreement; therefore the protocols do not require adjustment.

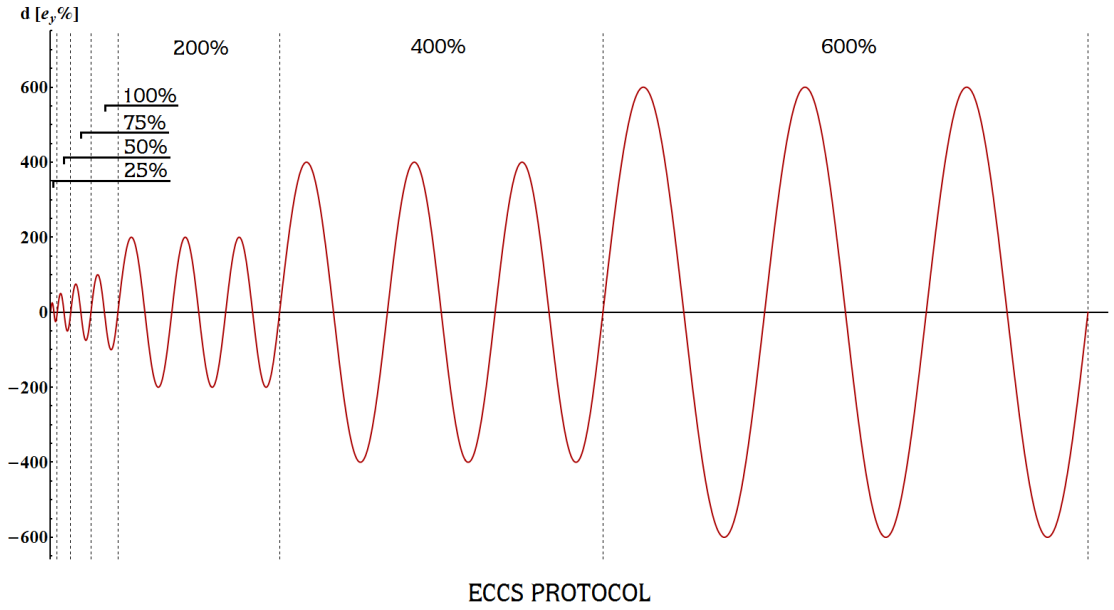

Figure 16 – Loading protocol specified in [4] 3.3

3.3. COMBINED PROTOCOL

A combination of the aforementioned protocols is used during the type tests (Figure 17). The number of load cycles in the combined protocol surpasses the requirements of both source protocols. The combined protocol enhances the evaluation of tests by providing more data about the specimens' behaviour and subjecting the BRBs to a more diverse set of load cycles, thus simulating actual seismic excitation in a more realistic manner.

After first yield, cycles with 7.5 mm and 10 mm target displacements are included. From then on displacements are increased in 5 mm increments until the design displacement is reached. 5 load cycles are planned at each intermediate displacement level, except the final, where a total of 30 load cycles are intended. The latter is not a necessary criterion that has to be reached to comply with requirements of EN 15129.

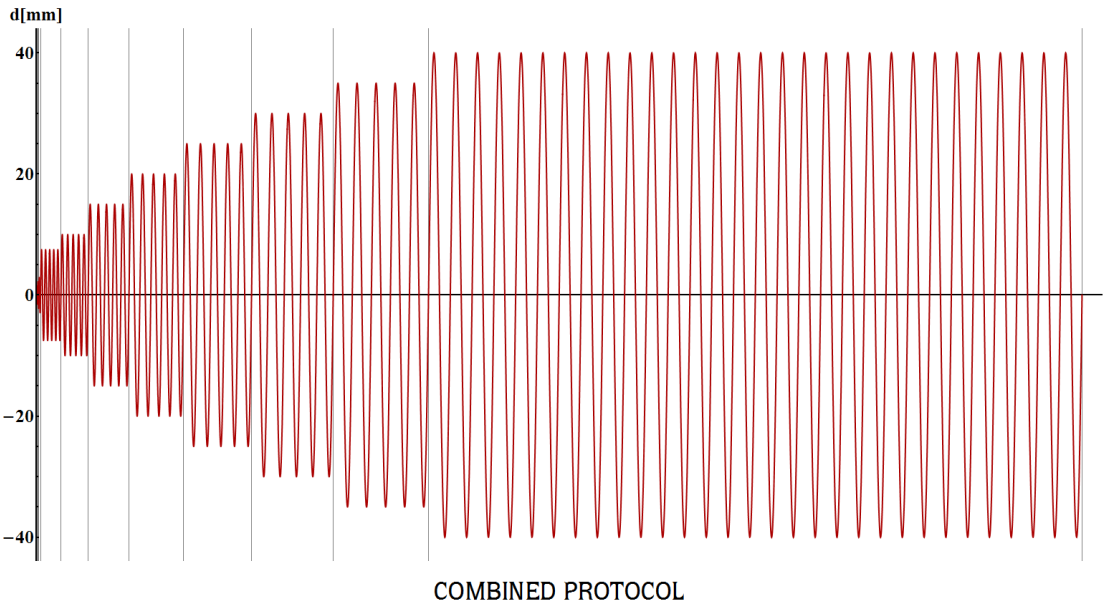

Figure 17 – Combined loading protocol

4. RESULTS & ANALYSIS

4.1. BEHAVIOUR IN ELASTIC RANGE – FIRST BRANCH STIFFNESS

According to the protocol shown in Section 3.3, testing is force-controlled before yielding. A total of four load levels are included, the fourth being the expected yield load that is increased during the tests as long as the specimens show elastic behaviour. Specimen behaviour before yielding is shown on Figure 18 for both tested BRB elements. According to the figure, behaviour of tested elements shows negligible variation in the elastic range.

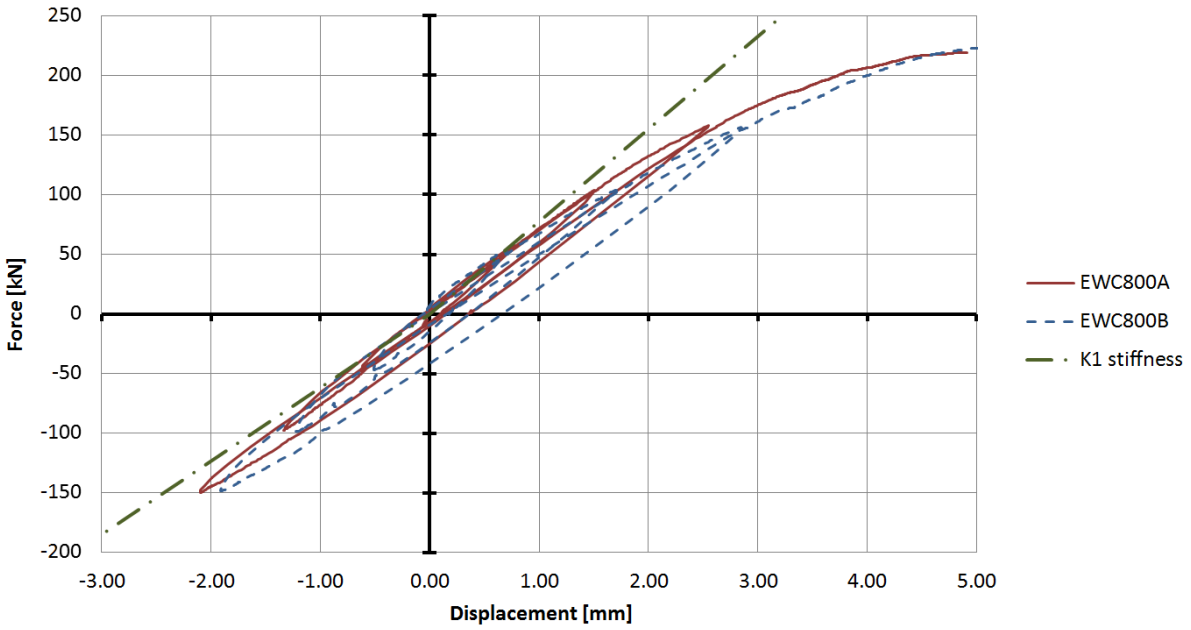

Figure 18 – Behaviour of BRB specimens before yielding

The so called first branch stiffness is identical to the initial stiffness of a nonlinear device and it is defined in EN 15129 as the following value:

$$K_1 = \frac{\frac{V_{Ebd}}{5} - \frac{V_{Ebd}}{10}}{d\left(\frac{V_{Ebd}}{5}\right) - d\left(\frac{V_{Ebd}}{10}\right)} \quad (2)$$

where:

V_{Ebd} is the force corresponding to d_{bd}, obtained in the 3rd load cycle

$d(x)$ is the displacement corresponding to force x

Using the aforementioned definition, the first branch stiffnesses for the tested specimens are shown in Table 2 with the data used for calculations also included. The force corresponding to design displacement is derived in Section 4.3.3. As the difference between behaviour under tension and compression in the elastic range is small, but not necessarily negligible, stiffness in both loading directions are calculated.

Table 2 – First branch stiffness of tested BRBs

	Tension				Compression				C/T
	A	B	mean	A/B	A	B	mean	A/B	
V_{Ebd} [kN]	320.1	327.2	323.7	97.8%	-432.4	-451.5	-442.0	95.8%	136.6%
$d(V_{Ebd}/10)$ [mm]	0.50	0.55	0.53	90.9%	-0.63	-0.71	-0.67	88.7%	127.6%
$d(V_{Ebd}/5)$ [mm]	0.98	1.12	1.05	87.5%	-1.31	-1.47	-1.39	89.1%	132.4%
K_1 [kN/mm]	66.35	57.19	**61.77**	116.0%	63.59	59.57	**61.58**	106.7%	99.7%

where:

A marks the results for EWC800A

B marks the results for EWC800B

mean is the mean value based on the available experimental data

A/B is the ratio of the results for the two specimens expressed in percentages

C/T is the ratio of the mean values for compressive and tensile loading expressed in percentages

4.2. FIRST YIELD

As already mentioned in the previous section, yielding is examined for both specimens under tensile loading. Under decreased loading speed, the loads are increased up to the point where displacements grow without significant change in load values.

4.2.1. ACTUAL CROSS-SECTION RESISTANCE

Actual cross-section resistance is defined using the actual yield strength of the steel material ($f_{ya,c}$) measured using tensile test in an independent laboratory (see Section 2.1). The following definition results in an elastic resistance of **225.6 kN**.

$$R_{el,c} = f_{ya,c} A_y \tag{3}$$

where:

$f_{ya,c}$ is the actual yield strength of the steel material

A_y is the cross-sectional area of the steel core in the yielding zone

The actual yield displacement (d_{ya}) is calculated by considering the changes in cross-sectional area in the steel core of the specimens. The yield displacement is the sum of deformations at each part of the steel core under $F_{ac,c}$ axial loading. Table 3 shows the details of calculation that result in an actual yield displacement of 3.121 mm.

Table 3 – Determination of actual yield displacement

	yielding zone	transition zone	elastic zone	sum
area [mm2]	800	1700	2600	
stress [MPa]	282	132.7	87	
strain [‰]	1.343	0.631	0.413	
length [mm]	2000	180	780	
deformation [mm]	2.686	0.113	0.322	**3.121**

4.2.2. YIELD FORCE AND DISPLACEMENT AS PER EN 15129

As per EN 15129 3.1.44 the coordinates of the intersection point of straight lines in the theoretical bilinear cycle define d_1 and V_1 values. Although these quantities are not explicitly called yield force and displacement in the standard, they are considered as such in this report, since they mark the border of inelastic behaviour. Section 4.3.10 shows the theoretical bilinear cycle for the EWC800 specimens. Since there is significant difference between the inelastic behaviour of buckling restrained braces under tension and compression, Table 4 shows separate values for V_1 and d_1 for each case.

Table 4 – Forces and displacements corresponding to the yielding points of the theoretical bilinear cycle

	V_1 [kN]	d_1 [mm]
Tension	**238.43**	**3.86**
Compression	**-255.56**	**-4.15**
C/T	107.2%	107.5%

4.2.3. YIELD FORCE AND DISPLACEMENT AS PER ECCS

Yield force and displacement are also calculated for each specimen using the recommendations of ECCS in [4]. Accordingly, knowing the initial stiffness ($K_{I,T}$) of the braces, a tangent is fitted to the experimental data with a gradient of $K_{I,T}/10$. Figure 19-20 shows the measured data and the resulting two tangents for each specimen. Coordinates of the tangents' intersection give the yield force and displacement. Resulting values for each specimen are summarized in Table 5.

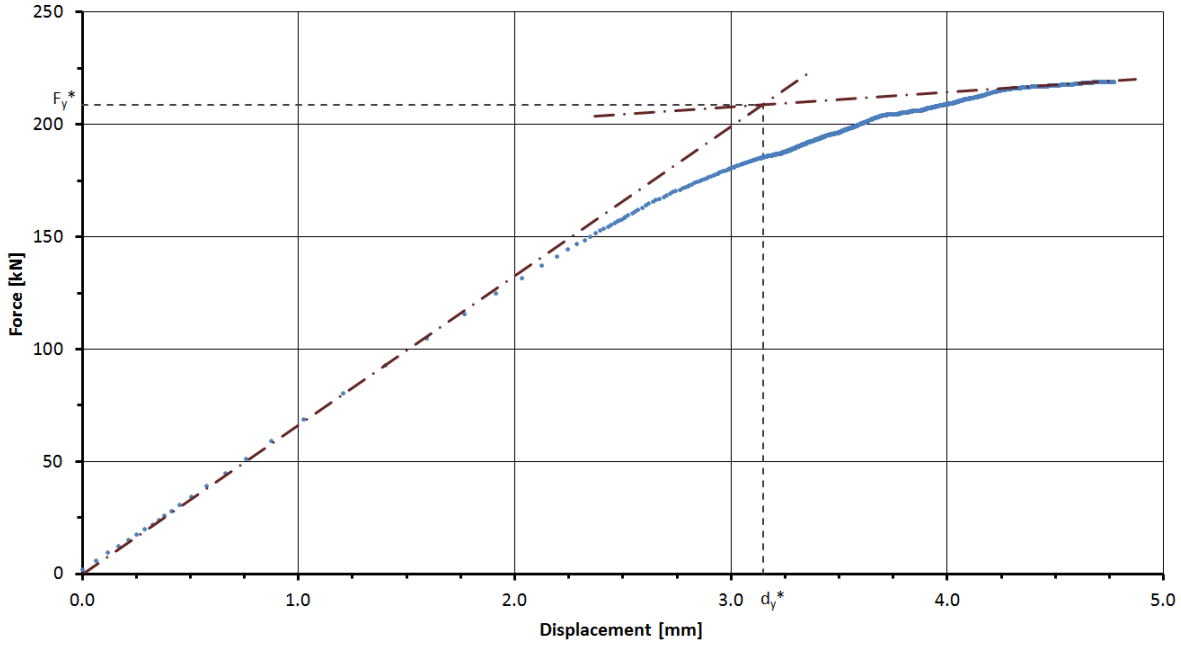

Figure 19 – Yield force and displacement determination for EWC800A

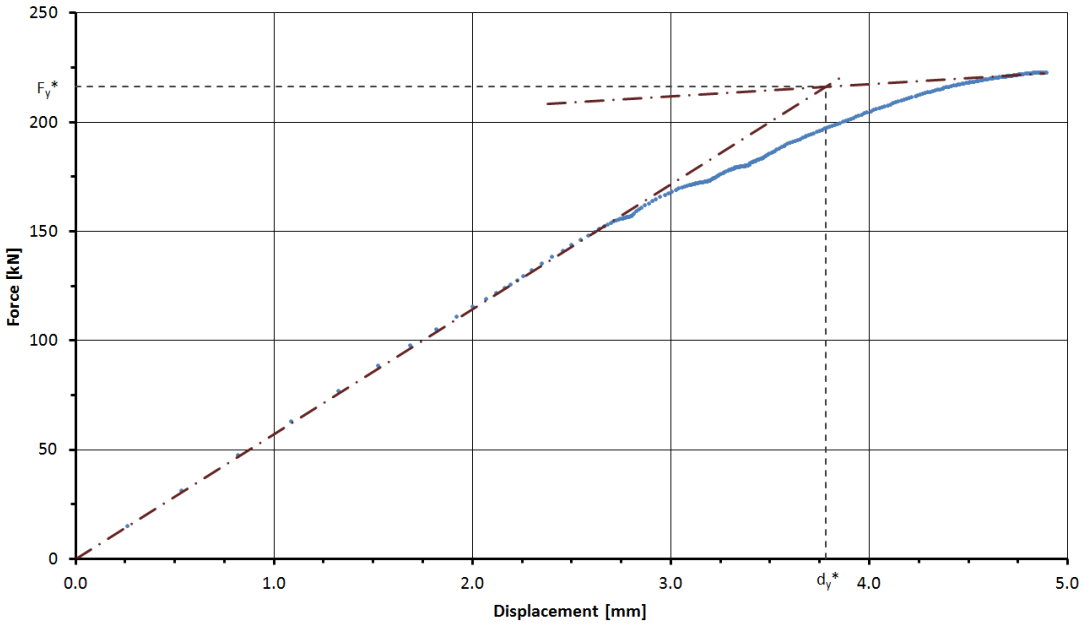

Figure 20 – Yield force and displacement determination for EWC800B

Table 5 – Yield force and displacement of tested BRBs

	F_y^* [kN]	d_y^* [mm]
EWC800A	208.79	3.15
EWC800B	216.23	3.78
mean	**212.51**	**3.47**
A/B	96.56%	83.33%

4.2.4. OVERSTRENGTH FACTOR

The overstrength factor (γ_{ov}) is calculated as the ratio of actual and characteristic yield strength. Actual yield strength ($f_{ya,c}$) is defined as the result of tensile tests done by an independent testing body (see Appendix B). The yield strengths used and the resulting overstrength factor are included in Table 6.

Table 6 – Overstrength factor of tested BRBs

$f_{yk,c}$ [MPa]	$f_{ya,c}$ [MPa]	γ_{ov}
235	282	**1.2**

4.3. POST-ELASTIC HYSTERETIC BEHAVIOUR

4.3.1. BEHAVIOUR

After yielding, specimens are subjected to displacement controlled cyclic loading at several amplitude levels according to the test protocol shown in Section 3.3. Both specimens show very stable behaviour under cyclic loading with no degradation. Gauges on the subassembly structures show that strains are within ±0.25‰, meaning that the examined elements remained elastic during the experiments. This verifies the expectation that yielding occurs only in the central so called yielding zone of the steel core and the other parts with significantly larger cross-sections remain elastic.

Both specimens reached the design displacement level and completed the intended loading protocol. Figure 21-22 show the hysteresis curves for each specimen. Following is a list of the properties calculated using experimental data with definition and detailed explanation of their calculation.

4.3.2. HYSTERETIC CURVES

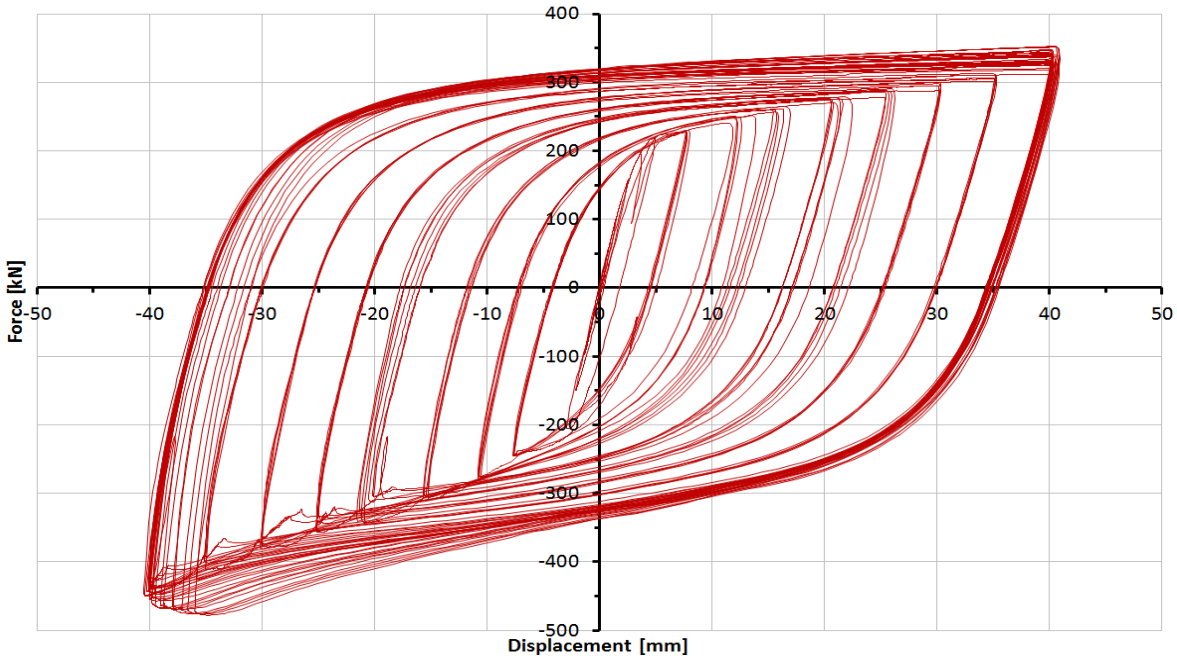

Figure 21 – Hysteresis loops for specimen EWC800A

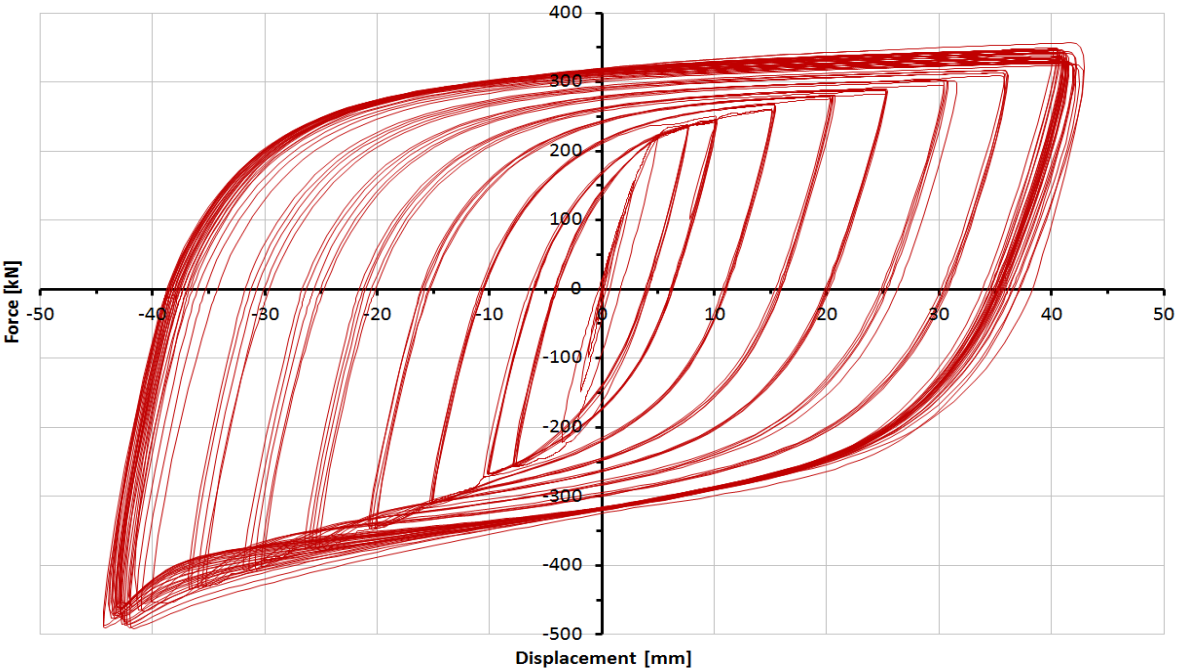

Figure 22 – Hysteresis loops for specimen EWC800B

4.3.3. DESIGN FORCE VALUE

As per EN 15129 3.1.7 the design force value (V_{bd}) is the force corresponding to the design displacement. The definition does not state which load cycle shall be taken into consideration when determining the force value. Since it is common practice in the standard to take the value from the 3rd load cycle as reference for several properties (e.g. second branch stiffness, effective damping etc.), the design force value is also determined using experimental data from the 3rd load cycle at d_{bd} displacement. This value is also referred to as V_{Ebd} in EN 15129 3.1.44.

Due to the special characteristics of buckling restrained braces, design force under tension ($V_{bd,T}$) considerably differs from the design force under compression ($V_{bd,C}$). Therefore both of them are determined and shown in Table 7 for each specimen.

Table 7 – Design force value for tested BRBs

	$V_{bd,T}$ [kN]	$V_{bd,C}$ [kN]
EWC800A	320.1	-432.4
EWC800B	327.2	-451.5
mean	**323.7**	**-442.0**
A/B	97.8%	95.8%

4.3.4. *SECOND BRANCH STIFFNESS*

As per EN 15129 3.1.34 second branch stiffness (also known as post-elastic stiffness) is defined as:

$$K_2 = \frac{V_{Ebd} - V(0.5d_{bd})}{0.5d_{bd}} \tag{4}$$

where:

$V(0.5d_{bd})$ is the force corresponding to $0.5d_{bd}$ in the 3rd load cycle with amplitudes of $0.5d_{bd}$

Since there is significant difference between the design force value under tension and compression (see Section 4.3.3), the value of second branch stiffness also depends on the direction of the axial load. Therefore $K_{2,T}$ is used for tensile and $K_{2,C}$ for compressive loading in this report.

Nonlinear Devices have to fulfil a set of requirements according to EN 15129 6.2 in order to assure stable behaviour under cyclic loading. The following requirement concerns the variation of second branch stiffness:

$$\kappa = \frac{|K_{2,i} - K_{2,3}|}{K_{2,3}} \leq 0{,}10 \qquad i > 1 \tag{5}$$

where:

$K_{2,i}$ is the second branch stiffness at the i-th loading cycle

Table 8-9 summarize the values of K_2 and $\varkappa$ for each specimen in each loading direction. Since the behaviour of tested specimens can be described as cyclic hardening (i.e. the second branch stiffness increases proportionally with the amount of energy dissipated), the variation in the value of $\varkappa$ is not the sign of instability, but the result of normal behaviour. Therefore the level of $\varkappa$ is considered acceptable. $K_{2,3}$ is taken as a representative value of second branch stiffness and is used in other calculations unless stated otherwise.

Table 8 – Second branch stiffness and its variation for EWC800A

EWC800A	Tension			Compression		
	$V_{bd,T,i}$ [kN]	$K_{2,T,i}$ [kN/mm]	$\varkappa_{T,i}$	$V_{bd,C,i}$ [kN]	$K_{2,C,i}$ [kN/mm]	$\varkappa_{C,i}$
$0.5d_{bd}$	273.9			-341.0		
2	318.2	2.21	0.04	-436.3	4.75	0.04
3	320.1	**2.30**		-432.4	**4.57**	
4	324.5	2.50	0.09	-435.4	4.72	0.03
5	324.9	2.52	0.10	-440.2	4.95	0.08
6	326.7	2.56	0.11	-443.1	5.06	0.11
7	325.2	2.55	0.11	-448.0	5.26	0.15
8	327.5	2.65	0.15	-422.7	4.09	0.10
9	328.6	2.69	0.17	-433.5	4.61	0.01
10	328.4	2.69	0.17	-439.0	4.94	0.08

Table 9 – Second branch stiffness and its variation for EWC800B

EWC800B	Tension			Compression		
	$V_{bd,T,i}$ [kN]	$K_{2,T,i}$ [kN/mm]	$\varkappa_{T,i}$	$V_{bd,C,i}$ [kN]	$K_{2,C,i}$ [kN/mm]	$\varkappa_{C,i}$
$0.5d_{bd}$	279.7			-348.3		
2	326.6	2.35	0.02	-466.6	5.92	0.02
3	327.7	**2.40**		-464.8	**5.83**	
4	328.7	2.45	0.02	-466.5	5.91	0.01
5	329.4	2.49	0.04	-459.2	5.55	0.05
6	329.9	2.51	0.05	-472.8	6.23	0.07
7	330.6	2.55	0.06	-464.6	5.82	0.00
8	332.8	2.66	0.11	-448.5	5.01	0.14
9	332.6	2.65	0.10	-461.4	5.66	0.03
10	334.6	2.75	0.14	-454.7	5.32	0.09

4.3.5. *EFFECTIVE STIFFNESS*

As per EN 15129 3.1.12 effective stiffness is defined as the secant stiffness at the design displacement of the device under examination:

$$K_{effb} = \frac{V_{Ebd}}{d_{bd}} \tag{6}$$

Since the design force value is different for tension and compression, two different effective stiffnesses are specified for each specimen. Table 10 shows the data used for calculation and the results.

Table 10 – Effective stiffness and its variation

	Tension			Compression			C/T
	$V_{Ebd,T}$ [kN]	d_{bd} [mm]	$K_{effb,T}$ [kN/mm]	$V_{Ebd,C}$ [kN]	d_{bd} [mm]	$K_{effb,C}$ [kN/mm]	
EWC800A	320.1	40	8.00	-432.4	-40	10.81	135.1%
EWC800B	327.2	40	8.18	-451.5	-40	11.29	138.0%
mean			**8.09**			**11.05**	136.6%
A/B			97.8%			95.7%	

4.3.6. *EFFECTIVE DAMPING*

As per EN 15129 3.1.10 the effective viscous damping of a device corresponds to the dissipated energy during cyclic response at the design displacement:

$$\xi_{effb} = \frac{W(d_{bd})}{2\pi V_{Ebd} d_{bd}} \tag{7}$$

where:

$W(d_{bd})$ is the energy actually dissipated by a device during the 3rd load cycle with d_{bd} maximum displacement

The above definition assumes that $V_{Ebd,C}=V_{Ebd,T}$, which does not hold in case of BRB elements. Therefore the expression is modified to take the difference in design force values into consideration:

$$\xi_{effb} = \frac{W(d_{bd})}{\pi(V_{Ebd,C} + V_{Ebd,T}) d_{bd}} \tag{8}$$

Nonlinear Devices have to fulfil a set of requirements according to EN 15129 6.2 in order to assure stable behaviour under cyclic loading. The following requirement concerns the variation of effective damping:

$$\Xi = \frac{\left|\xi_{effb,i} - \xi_{effb,3}\right|}{\xi_{effb,3}} \leq 0{,}10 \qquad i > 1 \tag{9}$$

where:

$\xi_{effb,i}$ is the effective damping at the i-th loading cycle

Table 11 summarizes the values of ξ_{effb} and Ξ for each specimen. Both specimens fulfil the above requirement in all loading cycles and shows high values of effective damping. $\xi_{effb,3}$ is taken as a representative value of effective damping and is used in other calculations unless stated otherwise. Since $\xi_{effb,3}$ is greater than 15% for both specimens, the tested BRB elements can be classified as Energy Dissipating Devices (EDD) as per EN 15129 D.1.

Table 11 – Effective damping values and their variation for the tested specimens

	EWC800A		**EWC800B**	
cycle	ξ_{effb} [%]	Ξ	ξ_{effb} [%]	Ξ
2	43.8	0.005	41.9	0.009
3	**44.1**		**42.3**	
4	44.2	0.002	42.2	0.002
5	43.9	0.003	42.6	0.007
6	44.1	0.001	41.4	0.021
7	43.7	0.010	42.1	0.003
8	45.2	0.025	43.2	0.023
9	44.5	0.009	42.4	0.003
10	44.4	0.007	43.5	0.028
11	44.5	0.011	42.5	0.006
12	44.6	0.012	42.1	0.003
13	44.3	0.004	42.0	0.006
14	44.1	0.001	42.7	0.009
15	44.2	0.002	43.1	0.018
16	44.2	0.003	43.5	0.029
17	44.2	0.004	41.4	0.020
18	44.0	0.003	42.1	0.004
19	44.3	0.005	42.7	0.011
20	43.9	0.004	42.3	0.000
21	44.1	0.002	42.4	0.004
22	44.1	0.000	40.9	0.033
23	43.8	0.006	42.7	0.009
24	44.1	0.000	44.3	0.047
25	44.0	0.002	42.3	0.000
26	44.2	0.003	41.7	0.013
27	43.8	0.006	41.9	0.009
28	44.3	0.005	42.2	0.002
29	44.2	0.002	41.7	0.014
30	44.2	0.003	41.7	0.014

The level of effective damping depends on the deformation the BRB element is subjected to. This relationship is shown on Figure 23. The following function is fitted to experimental data using least squares approximation:

$$\xi_{effb} = c \cdot \sqrt[5]{\epsilon_y^{pl}} \tag{10}$$

The dashed curve shows the above function with a c constant of 38.8. The figure shows that the level of effective damping is significant even at deformation levels below d_{bd} (2% strain).

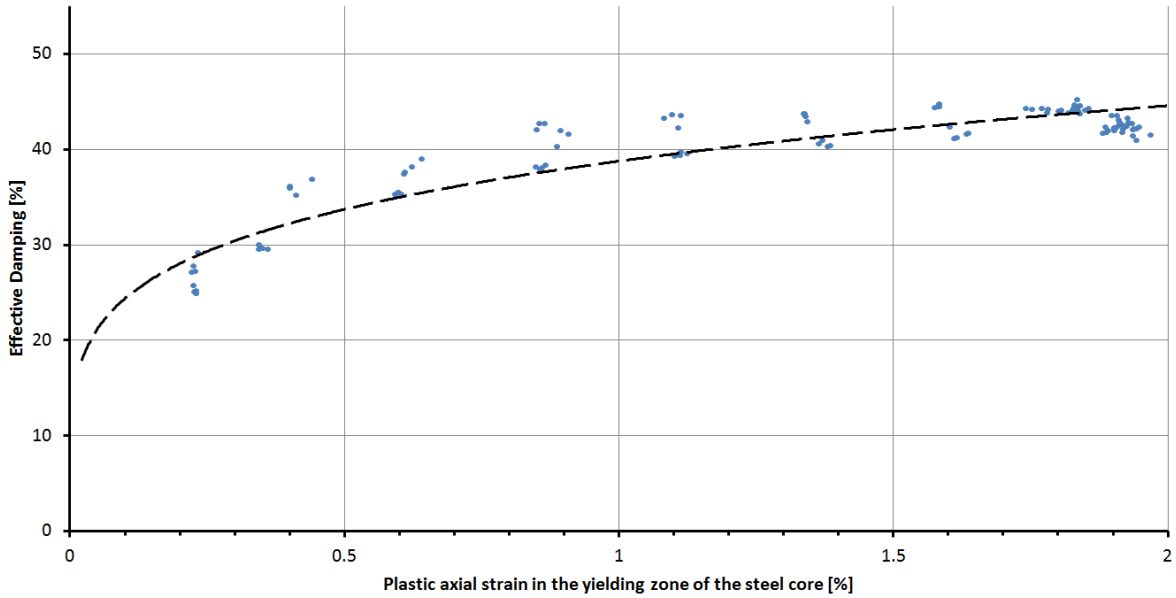

Figure 23 – Effective damping at different strain levels for the tested BRB elements

4.3.7. *ENERGY DISSIPATION CAPABILITY, CUMULATIVE INELASTIC DEFORMATION*

Apart from effective damping, the cumulative inelastic axial deformation capacity (η) is also addressed in this report. Although it is not included in EN 15129, this value is an important property of nonlinear devices, because it shows the energy dissipation capability of the device. It can be calculated as a ratio of total dissipated energy and elastic deformation energy:

$$\eta = \frac{E_h}{R_{el,c} d_{ya}} \tag{11}$$

where:

E_h is the total dissipated hysteretic energy

$F_{ac,c}$ is the actual cross-section resistance (see Section 4.2.1)

d_{ya} is the actual yield displacement (see Section 4.2.1)

Figure 24 shows the level of η versus the number of load cycles after yielding in the experiment. The final values significantly exceed the minimum requirements of both AISC (η>200) [5] and FEMA 450 (η>140) [6] provisions. These requirements are based on the cumulative brace deformation expected from a single design-level earthquake [7]. Based on these results, both tested braces are likely to be able to resist several consecutive earthquakes.

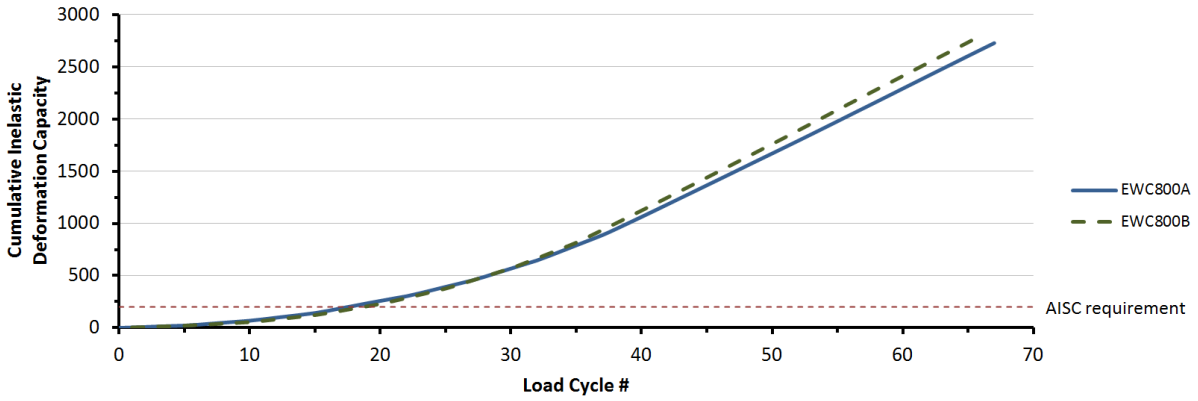

Figure 24 – Cumulative inelastic deformation capacity of tested specimens

4.3.8. *TENSION STRENGTH ADJUSTMENT FACTOR*

The tension strength adjustment factor accounts for strain hardening that causes the tensile strength of BRB elements to increase after each loading cycle. It is not yet included in EN 15129, therefore its definition below is based on AISC C16.2d:

$$\omega = \frac{V_{bd,T}}{f_{ya,c}A_y} = \frac{V_{bd,T}}{F_{ac,c}} \tag{12}$$

where:

$V_{bd,T}$ is the tension force corresponding to the design displacement

$f_{ya,c}$ is the measured (actual) yield strength of the steel core (see Appendix B)

A_y is the area of the steel core

$F_{ac,c}$ is the actual cross-section resistance (see Section 4.2.1)

The value of ω is required to be greater than 1.0 as per AISC C16.2d. According to the results shown in Table 12, both of the braces tested fulfil this requirement and the variation of ω is not significant.

Table 12 – Tension strength adjustment factor for tested BRBs

	$V_{bd,T}$ [kN]	$F_{ac,c}$ [kN]	ω
EWC800A	320.1	225.6	1.418
EWC800B	327.2	225.6	1.450
mean	323.7		**1.434**
A/B	97.8%		97.8%

4.3.9. *COMPRESSION STRENGTH ADJUSTMENT FACTOR*

The compression strength adjustment factor accounts for the compression overstrength (with respect to tension strength). It is not yet included in EN 15129, therefore its definition below is based on AISC C16.2d:

$$\beta = \frac{V_{bd,C}}{V_{bd,T}} \tag{13}$$

where:

$V_{bd,T}$ is the tension force corresponding to the design displacement

$V_{bd,C}$ is the compression force corresponding to the design displacement

The value of β is required to be greater than 1.0 as per AISC C16.2d. According to the results shown in Table 13, both of the braces fulfil this requirement and the variation of β is negligible.

Table 13 – Compression strength adjustment factor for tested BRBs

	$V_{bd,T}$ [kN]	$V_{bd,C}$ [kN]	β
EWC800A	320.1	-432.4	1.351
EWC800B	327.2	-451.5	1.380
mean	323.7	-442.0	**1.365**
A/B	97.8%	95.8%	97.9%

4.3.10. *THEORETICAL BILINEAR CYCLE*

As per EN 15129 3.1.44 the theoretical bilinear cycle (TBC) shall be used to identify the main mechanical characteristics of a Nonlinear Device. Gradients of the linear cycles are defined by the first and second branch stiffnesses. The intersection point of the two lines defines d_1 and V_1. This type of bilinear relationship is similar to the so called backbone curve in the USA with the intersection being the yielding point.

Figure 25 shows the TBC for the tested EWC800 specimens. The vertical axis shows the load bearing capacity, while the horizontal shows the deformation of the braces. Figure 26 shows the relationship between the TBC and the hysteresis curves by plotting both of them in the same coordinate system.

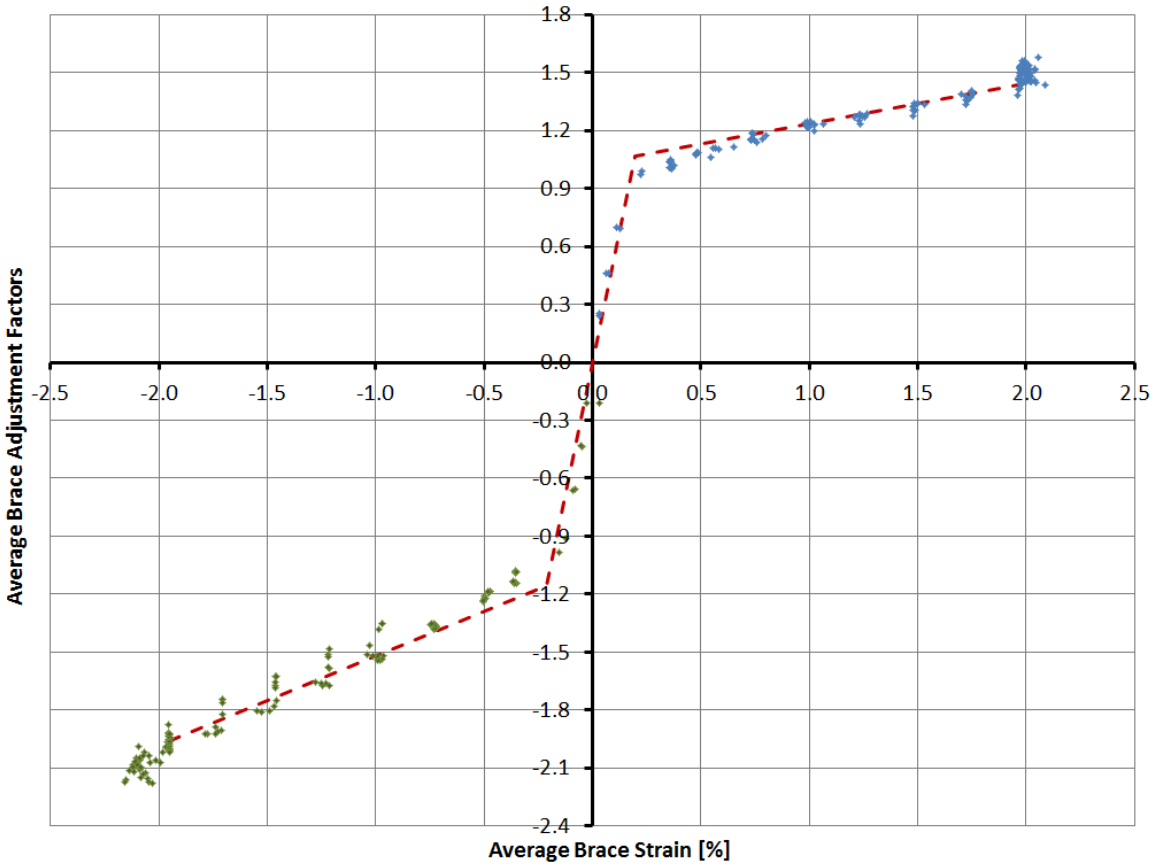

Figure 25 – Theoretical bilinear cycle for the EWC800 specimens

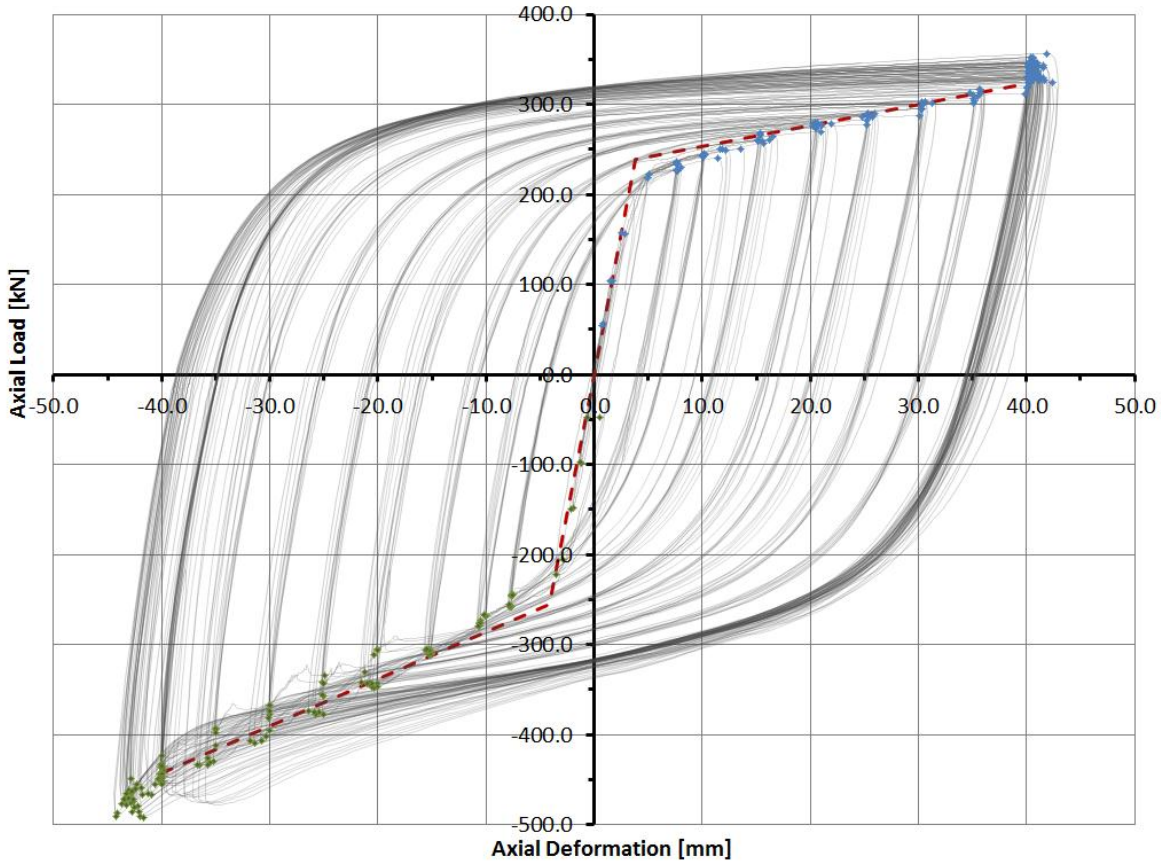

Figure 26 – Theoretical bilinear cycle and hysteresis curves for the EWC800 specimens

4.3.11. *ALTERNATIVE THEORETICAL BILINEAR CYCLE FOR DESIGN*

An alternative theoretical bilinear cycle is presented in Figure 25 which uses the expressions for tension and compression strength adjustment factors (see Sections 4.3.8, 4.3.9) to describe the nonlinear behaviour of the element. The vertical axis shows the load bearing capacity normed by the actual cross-section resistance determined in Section 4.2.1. The horizontal axis represents the strain in the yielding zone of the steel core.

This alternative TBC gives a better approximation of the behaviour of the steel core, especially when plastic deformations are small.

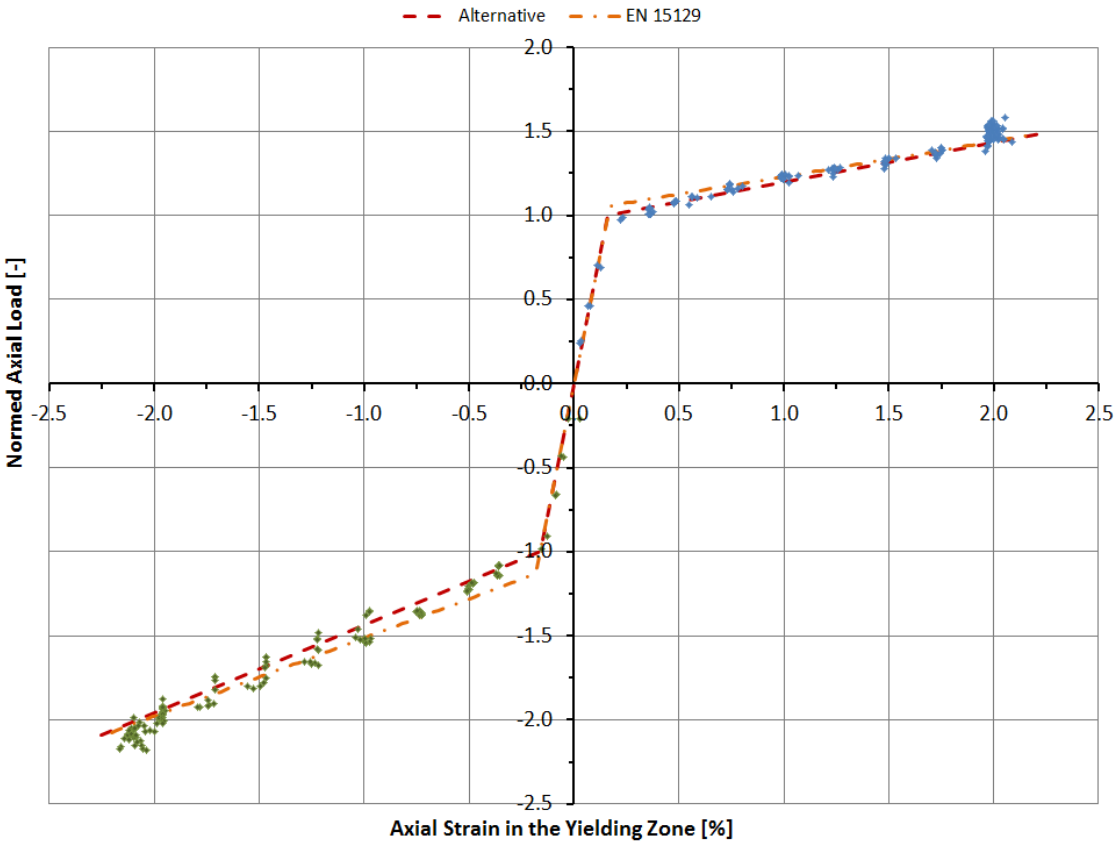

Figure 27 – Alternative bilinear cycle for design based on experimental results

4.4. FAILURE

Since the force-displacement capacity is also an important characteristic of displacement dependent devices in EN 15129, a quasi-ramp test was planned to be performed after completion of the pre-determined number of load cycles provided that the braces are in appropriate condition. After completing the test protocol for the EWC800A specimen, the brace is unloaded and examined for any visible damage or deterioration that might affect further examination. After finding no damages, the specimen is loaded monotonically by tensile load until failure. Results of this procedure are discussed in Section 4.4.1.

Repeating the quasi-ramp test for specimen EWC800B is considered unnecessary since only a single test is needed as per EN 15129 6.4.4 b) and the results of specimen EWC800A do not justify the need for another test. Therefore in case of the EWC800B specimen after finishing the loading protocol, cyclic loading at the design displacement level is continued until failure to see how far the limit of energy dissipation is. The specimen fails under tensile loading in the 2nd additional load cycle.

4.4.1. FORCE-DISPLACEMENT CAPACITY

As per EN 15129 6.2 the force-displacement capacity of a device is expressed by the $\gamma_b\gamma_x V_{Ebd}$ and $\gamma_b\gamma_x d_{bd}$ for loads and displacements, respectively.

where:

γ_b is a partial factor and its value for displacement dependent devices shall not be less than 1.1.

γ_x is a magnification factor also used in EN 1998-1 to increase the reliability of earthquake engineering structures. While minimum values of γ_x are specified for isolators, its value is not defined for devices that are not part of an isolation system. EN 1998-1 10.3 (2)P recommends a value of 1.2 for buildings.

Force-displacement capacity shall be measured until only one of the above criteria, the one that is reached first. Measurements according to EN 15129 6.4.4 b) shall be made using ramp tests. Since BRBs are displacement dependent devices with relatively low second branch stiffness, the displacement criterion is satisfied before the load criterion. Results of the monotonic loading that the EWC800A specimen is subjected after finishing the cyclic load test protocol are considered when describing the force-displacement capacity of the EWC800 specimens. Since the specimen has already dissipated a significant amount of energy before the monotonic loading, results of this test are inferior to those of a standard ramp test, where the specimen does not experience any loading beyond its yielding point before the test.

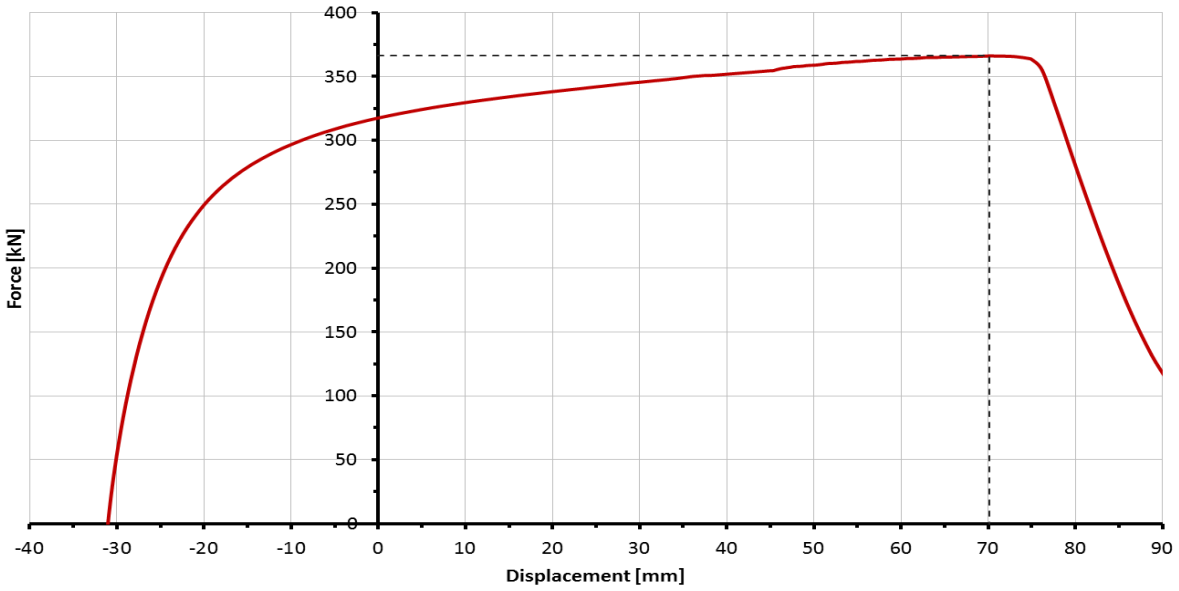

Figure 28 – Force-displacement curve of the monotonic loading phase of EWC800A

Figure 28 shows the force-displacement curve experienced during monotonic loading until failure at a displacement of **70.47 mm** and a maximum tensile load of **366.1 kN** (failure is defined as the point from where the gradient of the curve is no longer positive, meaning that displacement increases while the load level is no longer increasing). The design displacement value in the tests is 40 mm. The maximum displacement is 176.2% of the design displacement; thus the specimens have sufficient capacity for design with typical $\gamma_b\gamma_x$ values.

4.4.2. DISPLACEMENT CAPACITY (LATERAL FLEXIBILITY)

Lateral flexibility of the specimens is expressed as the maximum displacement and strain reached during the quasi-ramp test performed with specimen EWC800A. Maximum displacement (d_{max}) reached before failure is **70.47 mm**. At d_{max} displacement the total strain in the yielding zone of the steel core ($\varepsilon_{cy,max}$) is **3.47%**. Considering the specimen a single element with a length equal to the wp-wp length of the BRB, an equivalent maximal strain ($\varepsilon_{eq,max}$) is determined: **1.76%.**

4.4.3. *DISASSEMBLY*

Both specimens are disassembled by cutting them in half longitudinally and removing the ruptured steel core after failure. Several observations verify that the specimens' behaviour under cyclic loading is in line with theoretical expectations:

1. Remaining plastic deformation in the steel cores show that buckling does occur during the tests and judged by the wavelength higher modes are reached with several full sinusoidal waves visible on the core (Figure 29).
2. Looking at the other face of steel cores shows that considerable buckling occurs only around the weak axis. Cores look similar to their original shape when viewed from the direction of the strong axis (Figure 30). This can also be verified by examining the surface of the concrete housing the steel core: the buckled steel marked one face of the concrete at certain intervals while the other face shows no marking, meaning no buckling occurred in that direction (Figure 31).
3. Remaining parts of the steel core at the vicinity of rupture have a typical shape experienced when steel rods fail under uniaxial tensile loading (i.e.: the rupture surface is at an approximately 45 degrees angle from the original surface of the steel core, contraction of the cross-section is clearly visible), as Figure 32 shows.
4. Rupture occurs in the yielding zone, close to the midpoint of the steel core.
5. The elastic and transition zones of the steel core show no damage or impairment; therefore it is safe to conclude that these parts remain elastic during the tests (Figure 33).
6. No cracks or damage is apparent on the surface of the concrete that shall be separated from the steel core by the air gap. This leads to the conclusion that the concrete casing is not carrying axial loads, thus it is effectively decoupled from the steel core Figure 34.

Figure 29 – Visible residual plastic deformation showing that local buckling occurred around the weak axis

Figure 30 – No sign of residual deformation from local buckling around the strong axis

Figure 31 – The face of the concrete casing is clearly marked by the buckled steel core

Figure 32 – Rupture surface of the steel core

Figure 33 – Elastic and transition zones of the steel core show no damage

Figure 34 – Close-up view of the concrete surface shows no cracks or damage

4.5. SUMMARY OF IMPORTANT CHARACTERISTICS

Table 14 summarizes the parameters used to describe the behaviour of tested specimens in different aspects. All performance characteristics are based on Section 4 of this report.

Table 14 – Summary of important characteristics

Essential Characteristics	Notes	Property	
Load bearing capacity		$V_{bd,T}$ [kN]	323.7
		$V_{bd,C}$ [kN]	442.0
Stiffness	design value in kN/m	$K_{1,T}$ [kN/m]	61770
		$K_{1,C}$ [kN/m]	61580
		$K_{2,T}$ [kN/m]	2350
		$K_{2,C}$ [kN/m]	5200
		$K_{effb,T}$ [kN/m]	8090
		$K_{effb,C}$ [kN/m]	11050
Energy dissipation capability	equivalent damping value in percentage	$\xi_{eff,b}$ [%]	43.2
Lateral flexibility		d_{max} [mm]	70.47

REFERENCES

1. EN 1998-1:2008 *Design of structures for earthquake resistance – Part 1: General rules, seismic actions and rules for buildings*. European Committee for Standardization (CEN); 2008.
2. EN 15129:2010 *Anti-seismic devices*. European Committee for Standardization (CEN); 2010.
3. EN 10002-1:2001 *Metallic materials. Tensile testing. Part 1: Method of test at ambient temperature*. European Committee for Standardization (CEN); 2001.
4. *Recommended Testing Procedure for Assessing the Behaviour of Structural Steel Elements under Cyclic Loads*. European Convention for Constructional Steelwork – Technical Committee 1 – Structural Safety and Loadings – Technical Working Group 1.3 – Seismic Design; 1986.
5. ANSI/AISC 341-05 *Seismic Provisions for Structural Steel Buildings*. American Institute of Steel Construction (AISC); 2005.
6. FEMA 450-1/2003 NEHRP *Recommended Provisions for Seismic Regulations for New Buildings and Other Structures*. Buildings Seismic Safety Council (BSSC); 2003.
7. Fahnestock LA, Sause R, Ricles JM, Lu LW. Ductility demands on buckling-restrained braced frames under earthquake loading. *Earthquake Engineering and Engineering Vibration* 2003; 2(2): 255-268.

APPENDIX A: SPECIMEN DRAWINGS

The following pages are copies of specimen drawings
provided by Star Seismic Europe Ltd.

1 PC.
M=1:10
S235-SSE

CORE

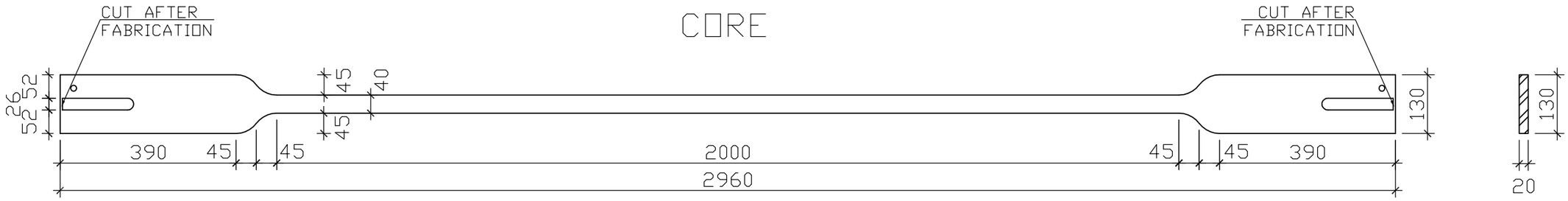

CORE DETAIL, M=1:5

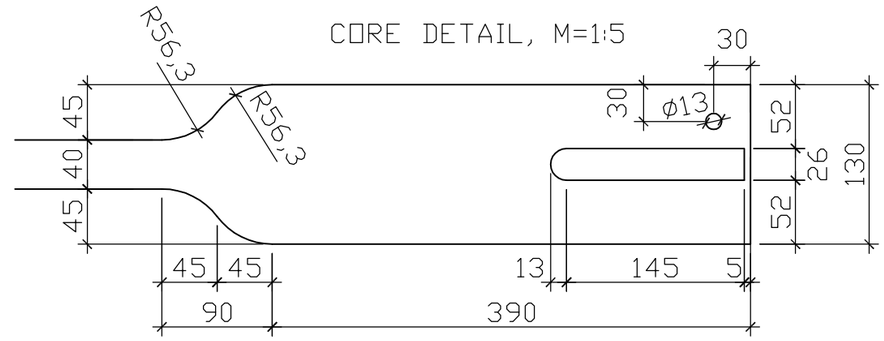

1 PC.
M=1:10
S355

TUBE

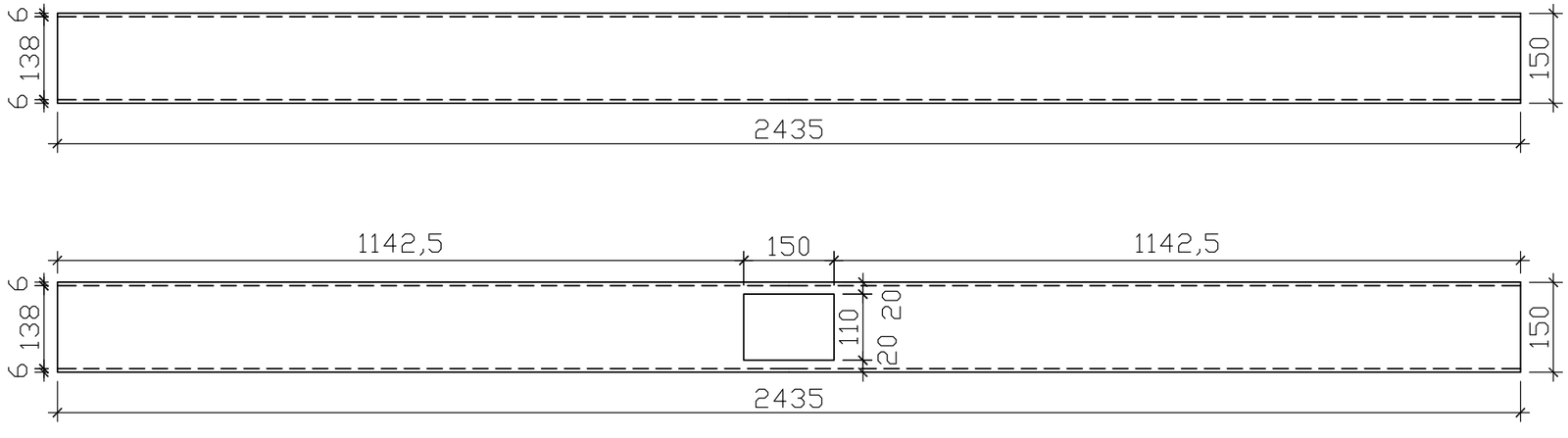

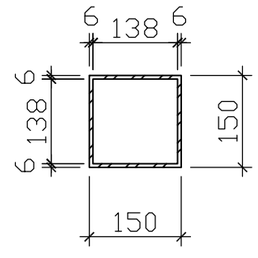

Designer: A Pohl	Project: Prototype Test Budapest University of Technology and Economics	Project no.: SSE P02		Revision:			
				Sign:	Note:	Date:	Rev. by:
Drafter: T Futo		Product no.: TS3, TS4					
Checked by: Z Bago	Product: CORE, TUBE	Drawing no.: SSE P02-01	Date: Sept. 24, 2010		Approved	Sept. 27, 2010	Z Bago

STAR SEISMIC Europe
www.starseismic.eu

COLLAR END PLATE

2 PCS.
M=1:5
S355

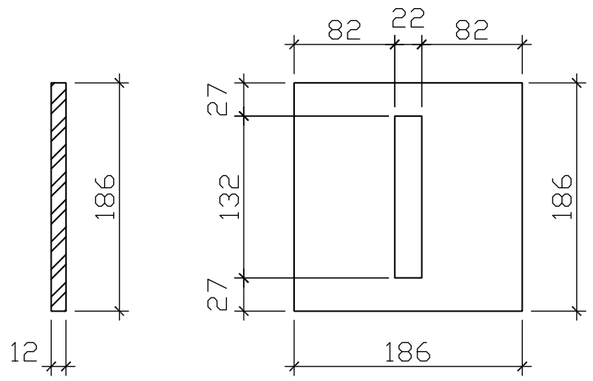

COVER

1 PC.
M=1:5
S355

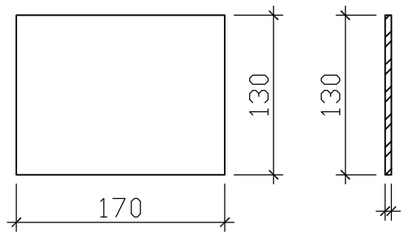

GUSSET END PLATE

2 PCS.
M=1:5
S355

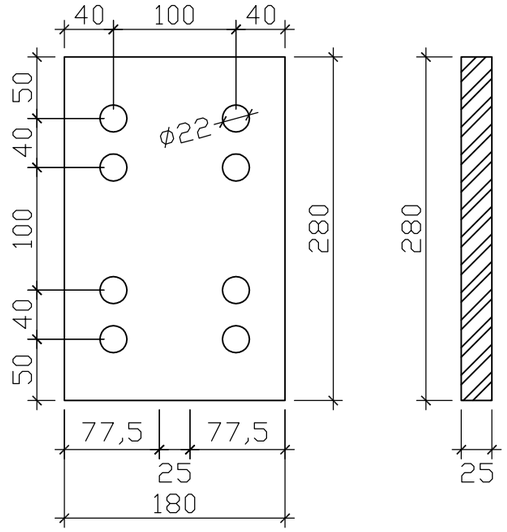

GUSSET PLATE

2 PCS.
M=1:5
S355

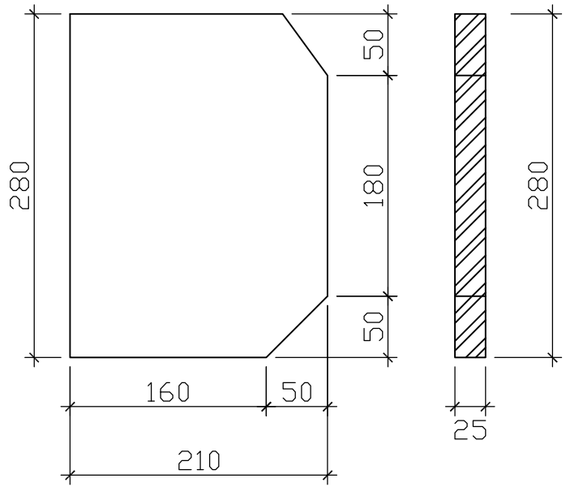

COLLAR ASSEMBLY

2 PCS.
M=1:5
S355

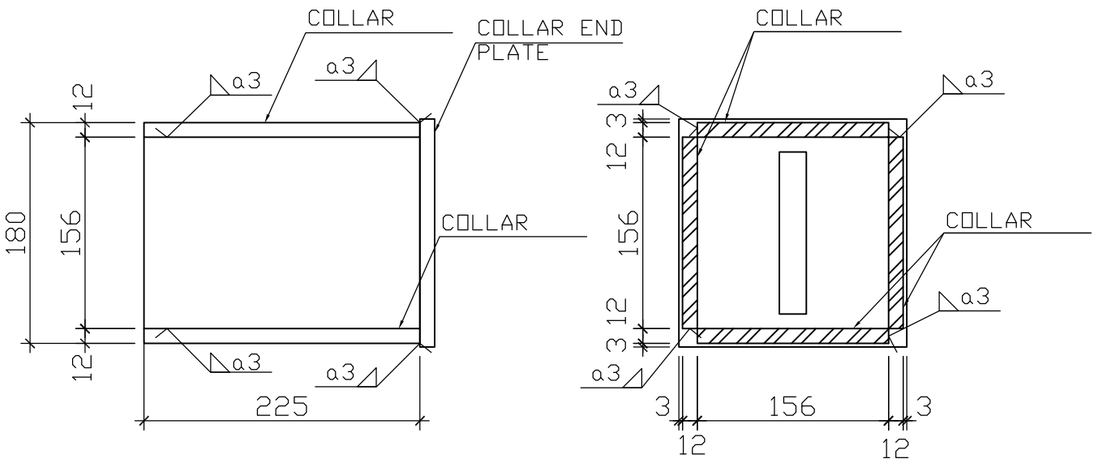

GUSSET PLATE ASSEMBLY

2 PCS.
M=1:5
S355

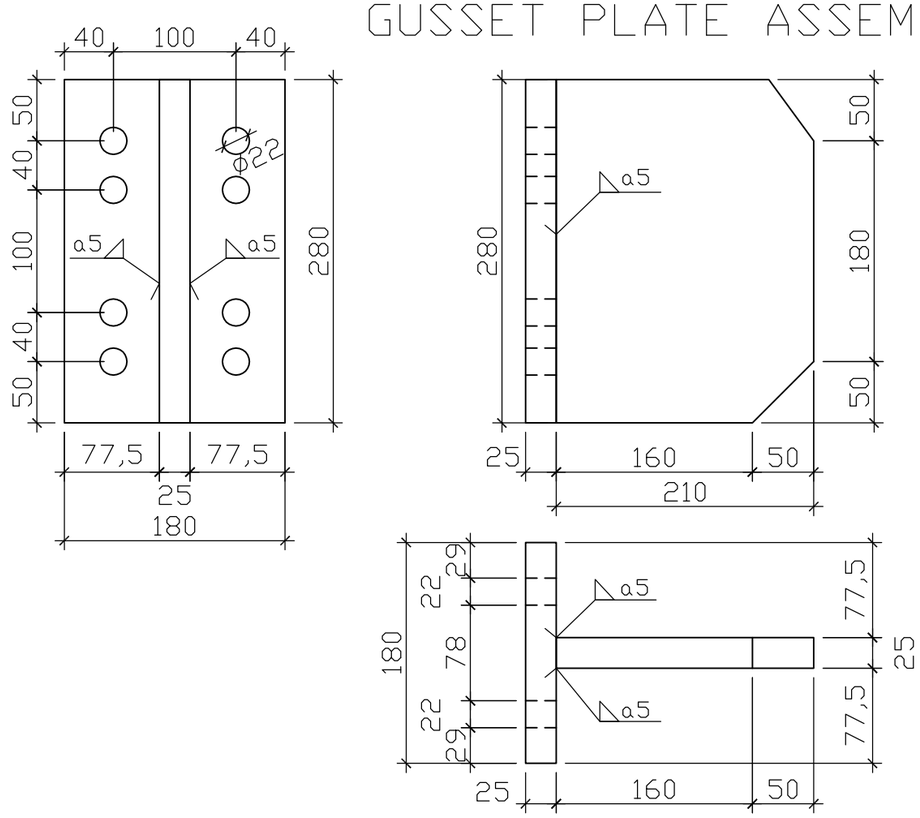

COLLAR SIDE PLATE

8 PCS.
M=1:5
S355

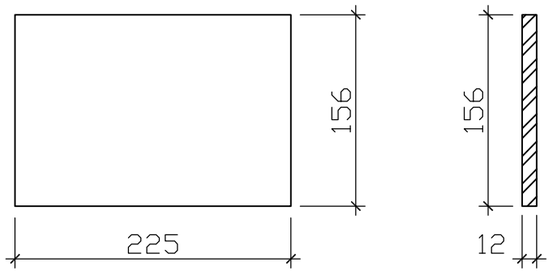

Designer: A Pohl	Project: Prototype Test Budapest University of Technology and Economics	Project no.: SSE P02		Revision:			
				Sign:	Note:	Date:	Rev. by:
Drafter: T Futo		Product no.: TS3, TS4					
Checked by: Z Bago	Product: COLLAR, COVER, GUSSET, END PL.	Drawing no.: SSE P02-02	Date: Sept. 24, 2010		Approved	Sept. 27, 2010	Z Bago

STAR SEISMIC Europe
www.starseismic.eu

M=1:10

BUCKLING RESTRAINED BRACE ASSEMBLY

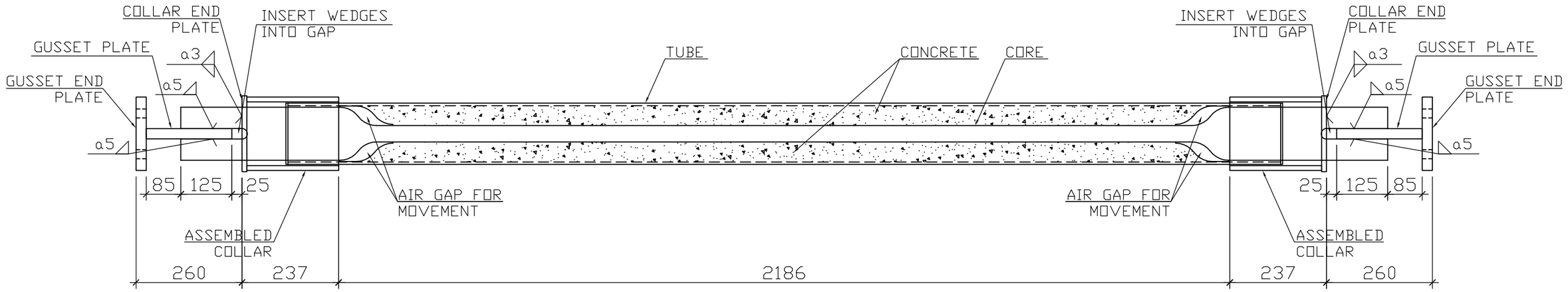

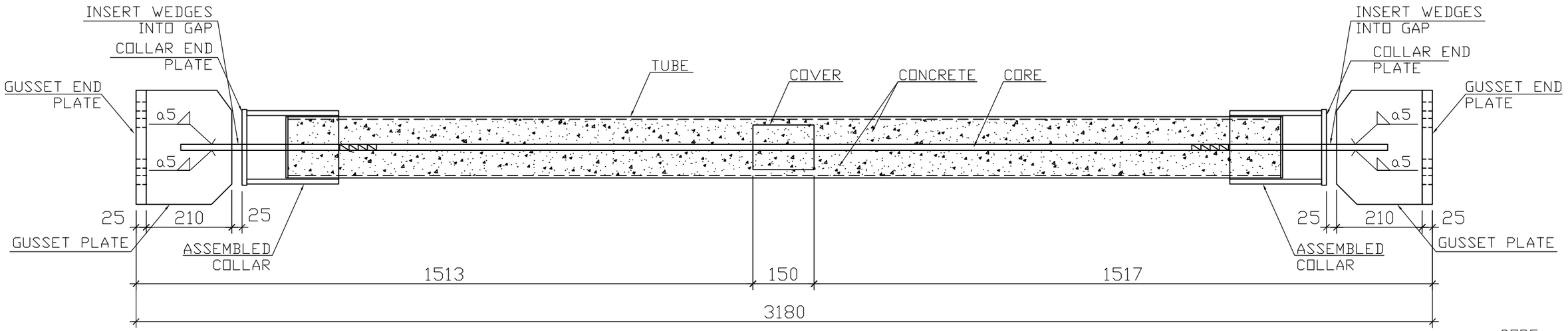

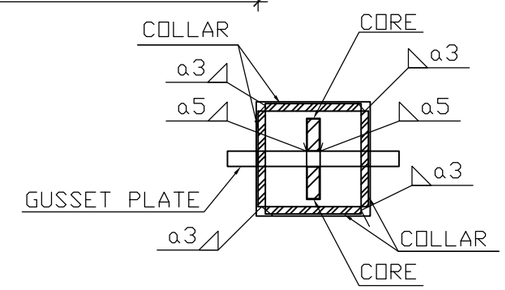

Designer: A Pohl	Project: Prototype Test Budapest University of Technology and Economics	Project no.: SSE P02		Revision:			
				Sign:	Note:	Date:	Rev. by:
Drafter: T Futo		Product no.: TS3, TS4					
Checked by: Z Bago	Product: BRB ASSEMBLY	Drawing no.: SSE P02-03	Date: Sept. 24, 2010		Approved	Sept. 27, 2010	Z Bago

STAR SEISMIC Europe
www.starseismic.eu

APPENDIX B: MATERIAL TEST REPORTS

The following pages are scanned copies of test reports
from independent testing bodies.

AGMI Material Testing and Quality Management Pte Co. Ltd.
H-1751 Budapest, P.O.Box. 114. Phone: (36)1 276-8945 Fax: (36)1 276-8650
E-mail: agmivig@agmi.hu

TEST PROTOCOL

Subject:	**Tensile test of specimens made from 20 mm thick steel plate**
Name of the Customer:	Star Seismic Europe Ltd.
Address and telephone of the Customer:	7960 Sellye, Vasút u. 17/a.
Person in charge at the Customer's side:	Bagó Zoltán ☎ (+36-30) 630-3037
No. of Order:	-
Department Carrying out the Test:	Mechanical and Analytical Testing Laboratory
Telephone:	(+36-1) 277-4901
E-mail:	agmimech@agmi.hu
Person in charge at AGMI Pte Co. Ltd.:	Majoros András
Test No.:	**1699**
Work No.:	10 – 210 – L – 00 / 1699
Place of examination:	Mechanical Testing Laboratory

Budapest, 15th November, 2010

AGMI Anyagvizsgáló és Minőségellenőrző ZRt Mechanikai és Analitikai Vizsgálati Laboratórium

Majoros András
Head of Laboratory

Rózsavölgyi Zsolt
Deputy Head of Laboratory

This Test Protocol contains two numbered pages in total.

Testing Laboratory is accredited by National Accreditation Service on No. NAT-1-1132/2010

Based on your order we have finished the requested tensile test of the 5 + 3 specimens made from 20 mm thick steel plate.

Identification data of the specimens:

A11, A12, A15 – manufactured by the Customer with plasma arc cutting
C1-C3, C11-C12 specimens – machined by AGMI Plant

According to the sampling sketch given by the Customer, samples C1-C3 were cross-directional, while all the others were longitudinal taking into consideration the original rolling direction.

The test was performed with MTS 810 type electro hydraulic tensile testing machine applying load rate control. The adjusted test speed was 2.5 kN/s.

The standard took into consideration during the test: MSZ EN 10002-1:2001. The yield strength was determined with electronic extensometer.

Together with the test results we also attach the Excel table which contains the acquired data and diagrams measured by the computer connected to the testing machine.

The calculated data of the test are summarized in Table 1.

Table 1.

Mark of the specimen	Thickness of the specimen	Width of the specimen	Yield strength $R_{p0,2}$	Tensile strength R_m	Elongation A
	mm		N/mm^2		%
A11.	20.23	25.2	280	448	35.5
A12.	20.01	25.6	283	451	36.0
A15.	20.15	25.2	282	450	37.0
C1.	20.33	25.3	291	429	31.0
C2.	20.23	25.2	292	433	30.0
C3.	20.10	25.3	287	432	35.0
C11.	20.30	25.3	290	432	33.5
C12.	20.27	25.2	291	431	33.0